

*Lewis*

**NASA  
Technical  
Paper  
2676**

March 1987

# Lewis Inverse Design Code (LINDES)

## *Users Manual*

Jose M. Sanz

(NASA-TP-2676) LEWIS INVERSE DESIGN CODE  
(LINDES): USERS MANUAL (NASA) 67 p CSCL 01A

N87-20238

Unclassified  
H1/02 45312



**NASA  
Technical  
Paper  
2676**

1987

Lewis Inverse Design  
Code (LINDES)

*Users Manual*

Jose M. Sanz

*Lewis Research Center  
Cleveland, Ohio*

## Contents

	Page
Summary .....	1
Introduction .....	1
Description of the Method .....	1
Hodograph Complex Equations .....	1
Elliptic Conformal Transformation .....	2
Numerical Solution .....	4
Boundary Layer Correction .....	5
Design Procedure .....	6
Appendices	
A—Input Data .....	8
B—Output List .....	10
Supercritical Propeller.....	10
Supercritical Rotor Blade.....	20
High Stagger Subcritical Rotor.....	30
Subcritical Turbine Blade.....	36
Supercritical Turbine Blade .....	45
Turning Vane .....	54
References .....	63

## Summary

The method of complex characteristics and hodograph transformation for the design of shockless airfoils was introduced by Bauer, Garabedian, and Korn and has been extended by the author to design subcritical and supercritical cascades with high solidities and large inlet angles. This new capability was achieved by introducing a new conformal mapping of the hodograph domain onto an ellipse and expanding the solution in terms of Tchebycheff polynomials. A new computer code, the NASA Lewis inverse design code, was developed based on this idea.

This new design code is an efficient method for the design of airfoils in cascade. In particular, the design of subcritical cascades of airfoils is a very fast, robust, and versatile process. The inverse design code can be made to interact with a turbulent boundary layer calculation to obtain airfoils with no separated flows at the design condition.

This report is intended to serve as a users manual for this design code. Material previously reported by the author is included here for completeness and quick access to the user. The manual contains a description of the method followed by a discussion of the design procedure and examples. The input parameters necessary to run the code are then described and their default values are given. Output listings corresponding to six different blade shapes designed with the code are given, as well as the necessary input data to reproduce the computer runs. The examples have been chosen to show that a wide range of applications can be covered with the code, ranging from supercritical propeller sections to wind tunnel turning vanes that can operate with a large inlet flow angle range.

## Introduction

This manual describes a new design technique, the NASA Lewis inverse design code (LINDES), based on the complex characteristics method and a new conformal mapping of the hodograph domain onto an ellipse (refs. 1, 2). This new mapping leads naturally to the use of Tchebycheff polynomials, to construct the solution of the equations. The equations of flow are integrated along a set of paths which are in accord with the topology that the elliptic mapping introduces. (Contact COSMIC, The University of Georgia, Athens, GA. 30602, concerning the availability of this program.)

The method of complex characteristics and hodograph transformation developed by Bauer, Garabedian, and Korn (ref. 3) has been widely used to design supercritical wing sections and cascades. With this method, excellent shockless airfoils have been designed and tested in this country and abroad. In its latest version, the method solves the problem of finding a shockless airfoil with a given pressure distribution.

Because of the conformal mapping used by Bauer, Garabedian, and Korn to transform the hodograph domain of the flow onto a circle, a restriction exists in their method which does not allow the design of cascades with high solidities. Also, a poor resolution at the leading and trailing edge regions may arise, in cases of high incidence angles, as a consequence of this mapping.

The heuristic idea behind the elliptic mapping is as follows: When the flow is mapped onto a circle, the upstream and downstream points of infinity are mapped into two interior points of the circle, where two logarithmic singularities of the solution, a source and a sink, are located. Increasing the separation between these two points reduces the gap-to-chord ratio. The limiting case of infinite gap-to-chord ratio, or the isolated airfoil, corresponds to the case in which both singularities coalesce. The two singularities can be more widely separated by mapping the flow onto an ellipse, further reducing the gap-to-chord ratio. A parameter related to the eccentricity of the ellipse will be introduced to control the solidity of the cascade.

High solidities have been achieved with this new method. A good resolution of points defining the body is obtained both at the leading and trailing edge regions, and larger incidence angles with thinner airfoils can be achieved. The method of complex characteristics, as applied to our problem, is reviewed in the following section.

## Description of the Method

### Hodograph Complex Equations

The equations of potential flow in hodograph coordinates can be described by the Chaplygin system,

$$\begin{aligned}\varphi_q &= \frac{M^2 - 1}{\rho q} \psi_\theta \\ \varphi_\theta &= \frac{q}{\rho} \psi_q\end{aligned}\tag{1}$$

in which  $\varphi$  and  $\psi$  are the potential and stream functions;  $M$  is the local Mach number;  $q$  and  $\theta$  are respectively the modulus and argument of the velocity vector, and  $\rho$  is the density. This system of equations is of mixed type, elliptic and hyperbolic, in the transonic regime.

In the method of complex characteristics, the variables are analytically extended into the four-dimensional domain of two complex variables, where the characteristic equations can always be solved. The system (eq. (1)) can be written in the canonical form (ref. 3)

$$\begin{aligned}\varphi_\xi &= \tau_+ \psi_\xi \\ \varphi_\eta &= \tau_- \psi_\eta\end{aligned}\quad (2)$$

where

$$\tau_\pm = \pm i \frac{\sqrt{1 - M^2}}{\rho}$$

The two independent variables  $\xi$  and  $\eta$  are arbitrary complex analytic functions of the characteristic coordinates

$$\begin{aligned}s &= \log h - i\theta \\ t &= \log h + i\theta\end{aligned}\quad (3)$$

where  $h$  is defined by

$$\begin{aligned}h(q) &= h(C_*) \exp \left( \int_{C_*}^q \sqrt{1 - M^2/q'} dq' \right) \\ h(C_*) &= \exp \left( \int_1^{C_*} \sqrt{1 - M^2/q'} dq' \right)\end{aligned}\quad (4)$$

and  $C_*$  is the critical speed.

Recall that the coordinates  $s$  and  $t$  are conjugated characteristic coordinates (ref. 3), in the subsonic domain. This means that, for subsonic points,  $s$  and  $t$  are complex conjugate numbers when  $q$  and  $\theta$  are real. If the variables  $\xi$  and  $\eta$  are defined in the form

$$s = f(\xi) \quad t = \bar{f}(\bar{\eta}) \quad (5)$$

with  $f$  analytic, then they are also conjugate coordinates. Under this transformation the sonic surface is mapped onto a curve of each characteristic plane, called the sonic locus (ref. 1).

The hodograph method is appropriate in solving an inverse problem. A solution is constructed with the correct logarithmic singularities, which represent a sink and source at infinity. The zero stream line, on the physical real plane, is the possible candidate for the body which generates the flow.

In the context of the complex system, equation (2), the correct mathematical problem to be solved is the characteristic initial value problem, where initial data are given in the two characteristic planes emanating from the initial point  $(\xi_0, \eta_0)$  in the four-dimensional space. Manipulation of this initial data can and has lead in the past (ref. 3) to the construction of shockless solutions. A new and fundamental approach in the application of hodograph methods was taken in reference 4, where the unknown domain of the flow is mapped onto the unit circle, by a conformal mapping of the type of equation (5). This allows for a systematic prescription of the initial characteristic data, based on a given pressure distribution over the airfoil. The next section describes how this idea is implemented.

### Elliptic Conformal Transformation

The transformation defined by equation (5) is used to map the flow onto an elliptic domain  $D$  of each coordinate characteristic plane. Because of this transformation, the coordinate characteristics are such that real subsonic points correspond to the domain of points of the form  $(\xi, \bar{\xi})$ , when  $\xi$  is a point enclosed by the portion of the boundary of  $D$ , where  $\xi$  and  $\eta$  are conjugate coordinates and the sonic locus. This part of the boundary will correspond to the subsonic part of the body. Points in the remainder of the domain  $D$  do not correspond to the real physical plane, and the real supersonic part of the body have to be found by searching for the zero stream line.

The elliptic domain and the corresponding Tchebycheff polynomials can be defined in the following form. Consider the conformal mapping

$$\omega = \frac{1}{2} \left( \xi + \frac{1}{\xi} \right) \quad 1 \leq |\xi| \leq R \quad (6)$$

of a circular ring in the plane onto the ellipse with axes defined by the points

$$\pm \frac{1}{2} \left( R + \frac{1}{R} \right) \pm \frac{1}{2} \left( R - \frac{1}{R} \right)$$

and the slit  $(-1, 1)$ . We consider the class of analytic functions in the ring which have a Laurent expansion of the form

$$F(\xi) = \sum_{-\infty}^{\infty} a_n \xi^n = \sum_{0}^{\infty} a_n \left( \xi^n + \frac{1}{\xi^n} \right) \quad (7)$$

in which  $a_n = a_{-n}$  for all positive  $n$ . The functions of the variable  $\omega$

$$T_n(\omega) = \frac{1}{2^n} \left( \xi^n + \frac{1}{\xi^n} \right) \quad n = 0, 1, 2, \dots \quad (8)$$

are actually the Tchebycheff polynomials of the first kind, as can be easily verified.

Observe that a function of equation (7) has the property

$$F(e^{i\theta}) = F(e^{-i\theta}) \quad 0 \leq \theta \leq \pi \quad (9)$$

This means that within this class of functions, points are identified with the same real part in the positive and negative parts of the unit circumference. Any analytic function on the ellipse in the  $\omega$ -plane can then be written in the form

$$F(\omega) = \sum_0^{\infty} a_n \left( \xi^n + \frac{1}{\xi^n} \right) = \sum_0^{\infty} a'_n T_n(\omega) = \sum_0^{\infty} b_n \omega^n \quad (10)$$

This shows that the ellipse is equivalent to the circular ring with the given identification of points on the unit circumference. This identification actually makes the slit introduced by the mapping (eq. (6)) unnecessary, making the elliptic domain singly connected.

The circular ring  $1 \leq |\xi| \leq R$  is adopted as the computational domain  $D$ , with the previous identification of points. The parameter  $R$  will control the eccentricity of the ellipse and, in this way, the solidity of the cascade. Several advantages arise from this formulation. The most important one is that Fast Fourier Transform (FFT) is able to compute the coefficients of the mapping function

$$f(\xi) = \sum_0^{\infty} a_n \left( \xi^n + \frac{1}{\xi^n} \right) \quad (11)$$

of the flow onto the computational domain  $D$ . Other advantages of this formulation will be discussed when the design procedure is described.

The supercritical design problem can be formulated as follows. Find an analytic solution

$$\begin{aligned} \varphi(\xi, \eta) &= R_e \{ \varphi_1(\xi, \eta) \log(\eta - \eta_1) \\ &\quad + \varphi_2(\xi, \eta) \log(\eta - \eta_2) + \varphi_3(\xi, \eta) \} \\ \psi(\xi, \eta) &= R_e \{ \psi_1(\xi, \eta) \log(\eta - \eta_1) \\ &\quad + \psi_2(\xi, \eta) \log(\eta - \eta_2) + \psi_3(\xi, \eta) \} \end{aligned} \quad (12)$$

of the system (eq. (2)), with  $\varphi_1, \varphi_2, \varphi_3$  and  $\psi_1, \psi_2, \psi_3$  regular functions, in the domain  $D$ , where the mapping function  $f$  defined by equation (11) satisfies the Dirichlet condition

$$R_e \{ f(\xi) \} = \log(h^*(\xi)) \quad |\xi| = R \quad (13)$$

and the stream function satisfies the boundary condition

$$R_e \{ \psi(\xi, \bar{\xi}) \} = 0 \quad |\xi| = R \quad (14)$$

The stream function is real valued for subsonic points, and the boundary condition (eq. (14)) is well defined when a proper branch of the solution is taken. The function  $h^*$  is defined by

$$h^*(q) = h(C_*) \exp \left( k \left| \int_{C_*}^q \sqrt{1 - M^2} dq' / q' \right| \right) \quad k > 0 \quad (15)$$

The regular part of the solution can be expanded as a linear combination of particular solutions obtained by taking as initial characteristic data a complete set of orthonormal functions, namely the Tchebycheff polynomials. The coefficients of this linear combination are then determined by imposing the boundary condition (eq. (14)). This boundary value problem has been proved to be well posed when the system of equations (1) is reduced to the Tricomi equation (ref. 5), that is, in the case of the transonic small disturbance equation. In the general case of the full potential equation that is dealt here, a low condition number for the matrix associated with the linear system in question, both when the domain  $D$  is a circle or an ellipse, indicates the well posedness of the problem.

With the definitions given,  $h^*$  and  $h$  become identical in the subsonic part of the domain  $D$ , where the parameter  $k$  is taken equal to unity. In the remainder of this domain,  $h$  is not real and the introduction of the function  $h^*$  becomes necessary. The consequence of using this Dirichlet condition is that the designed airfoil will not achieve the prescribed pressure distribution on the supersonic part of the airfoil.

The boundary conditions (eqs. (13) and (14)) are nonlinearly coupled. The nonlinearity of the problem arises from the fact that the speed distribution is given as a function of the arc length, and in equation (13) it is needed as a function of the coordinate  $\xi$  on the boundary  $|\xi| = R$ . The relationship between  $\xi$  and the arc length  $s$ , can only be determined when the potential function is known. On the other hand, the solution of the boundary value problem (eq. (14)) is linked to the knowledge of the mapping function  $f$ . An iterative procedure is then needed to solve the problem.

This iterative procedure is established by first computing an incompressible solution  $\varphi(\xi), \psi(\xi)$  on the elliptic domain, in terms of classic Jacobi elliptic functions. The incompressible solution is conformal invariant. The relation between the arc length  $s$  and the boundary variable  $\xi = Re^{i\theta}$  can then be established as  $\varphi(s)$  is known. This allows computation of the mapping function  $f$ , with the use of FFT, to solve the Dirichlet problem (eq. 13) with prescribed values of  $h^*$  at a number  $N$  of equidistant nodes on the circumference of radius  $R$ .

Once the mapping function is known, the system of equations (2) can be integrated, as  $\tau_{\pm}$  are, then, known functions of the variables  $\xi$  and  $\eta$ . Note that at each iteration an analytic solution is found. If the zero stream line is not self-intersecting and has the proper closure at the trailing edge, it represents a shockless airfoil.

## Numerical Solution

This section concentrates on the problem of finding a solution of the type of equation (12) to the system of equations (2), once the mapping function  $f$  has been determined. The notation

$$L_\xi(\varphi, \psi) = \varphi_\xi - \tau_+ \psi_\xi$$

$$L_\eta(\varphi, \psi) = \varphi_\eta - \tau_- \psi_\eta$$

is introduced. The requirement that the functions of equation (12) be solutions of the system of equations (2) with the pairs  $(\varphi_i, \psi_i)$  ( $i = 1, 3$ ) being regular functions leads to the homogeneous system, for each value  $i = 1, 2$  of the index  $i$ ,

$$\begin{aligned} L_\xi(\varphi_i, \psi_i) &= 0 \\ L_\eta(\varphi_i, \psi_i) &= 0 \end{aligned} \quad (16)$$

with

$$\varphi_i = \tau_+ \psi_i \text{ on } \eta = \eta_i \quad (i = 1, 2) \quad (17)$$

and to the inhomogeneous system

$$\begin{aligned} L_\xi(\varphi_3, \psi_3) &= 0 \\ L_\eta(\varphi_3, \psi_3) &= - \left( \sum_{i=1}^2 \frac{\varphi_i - \tau_+ \psi_i}{\eta - \eta_i} \right) \end{aligned} \quad (18)$$

The problem (eq. (16)) with the condition (eq. (17)) is known as the Riemann problem for that system. The solutions are the Riemann functions related to that problem and can be explicitly integrated along the characteristic  $\eta = \eta_i$ , in the form

$$\begin{aligned} \psi_i(\xi, \eta_i) &= \frac{C_i}{\sqrt{\tau_+(\xi, \eta_i)}} \\ \varphi_i(\xi, \eta_i) &= C_i \sqrt{\tau_+(\xi, \eta_i)} \quad (i = 1, 2) \end{aligned} \quad (19)$$

The complex constants  $C_1$  and  $C_2$  remain at our disposal. These two sets of Riemann functions can be integrated with a finite difference scheme that will be described later. On the  $\xi = \xi_i$ ,  $i = 1, 2$ , characteristics the initial data

$$\begin{aligned} \psi_i(\xi_i, \eta) &= \overline{\psi_i(\bar{\eta}, \bar{\xi}_i)} \\ \varphi_i(\xi_i, \eta) &= \overline{\varphi_i(\bar{\eta}, \bar{\xi}_i)} \end{aligned} \quad (20)$$

can be imposed.

Once these functions are determined, the inhomogeneous system (eq. (18)) can be integrated. For that, the solution is expanded in the form

$$\begin{aligned} \varphi_3 &= \varphi_3^{(o)} + \sum_1^N b_n \varphi_3^{(n)} \\ \psi_3 &= \psi_3^{(o)} + \sum_1^N b_n \psi_3^{(n)} \end{aligned} \quad (21)$$

Here  $(\varphi_3^{(o)}, \psi_3^{(o)})$  is a solution of the inhomogeneous problem (eq. (18)) with the the homogenous initial characteristic data

$$\psi_3^{(o)}(\xi, \eta_3) = \overline{\psi_3^{(o)}(\bar{\eta}_3, \bar{\xi})} = 0 \quad (22)$$

assigned on the two characteristics emanating from a point  $(\xi_3, \bar{\xi}_3)$ , which is subsonic and far from the singularities  $(\xi_1, \bar{\xi}_1)$  and  $(\xi_2, \bar{\xi}_2)$ . Each pair of functions  $(\varphi_3^{(n)}, \psi_3^{(n)})$  is a solution for the homogeneous system (eq. (16)), with the initial characteristic data

$$\psi_3^{(n)}(\xi, \eta_3) = \overline{\psi_3^{(n)}(\bar{\eta}_3, \bar{\xi})} = T_n(\omega), \quad n = 1, \dots, N \quad (23)$$

and where the  $T_n(\omega)$  are the Tchebycheff polynomials described in equation (8). Once each of these initial characteristic problems is numerically solved, the coefficients  $b_n$  on equation (21) can be determined by imposing the boundary condition (eq. (14)).

A rectangular grid is used to numerically solve each initial characteristic problem. Two sides of this rectangular grid are formed by two paths of integration, one in each characteristic plane. These paths allow the desired part of the flow to be computed. Three kinds of path of integration are used, subsonic, transonic, and supersonic paths. To reduce the amount of computation, the exterior circumference is divided into eight sectors, and the identical points  $(0, 1)$  and  $(0, -1)$  are always taken as initial point  $(\xi_3, \bar{\xi}_3)$ . From each singularity  $(\xi_1, \bar{\xi}_1)$  and  $(\xi_2, \bar{\xi}_2)$  a path is laid which goes directly to the point  $(\xi_3, \bar{\xi}_3)$  to compute the Riemann solutions. The corresponding  $\eta$ -path will be the complex conjugate of the  $\xi$ -path. Once the characteristics are reached through the point  $(\xi_3, \bar{\xi}_3)$ , the Riemann solutions plus the solution of the inhomogeneous problem (eq. (18)) are computed in the way described.

Subsonic paths are used in those sectors in which all the nodes are subsonic points. In this case the  $\eta$ -path is the complex conjugate of the  $\xi$ -path. As  $\xi$  and  $\eta$  are conjugate coordinates at subsonic points, the diagonal of the rectangle corresponds to real subsonic points. The initial data have been previously defined by the reflection laws (eqs. (20), (22), and (23)). In this form the computation can be reduced to the triangle below the diagonal. A path will consist, then, of a segment that starts at  $\xi_3$ , ends at the outer circle, and continues with the circular arc corresponding to the sector in question.

Transonic paths are used in those sectors below the sonic locus, where all, or some, of the nodes do not correspond to real subsonic points. The idea is that to reach those points beyond the sonic line, the two-dimensional manifold formed by the two paths has to avoid the sonic surface  $M(\xi, \eta) = 1$ , where the equations become ill conditioned. So, in the case of those paths, the  $\xi$ -path and the  $\eta$ -path should not be conjugates of each other. The idea is, as in reference 3, to traverse the corresponding sector in opposite directions for each path.

Finally, the supersonic paths compute the real supersonic zone of the body. These supersonic paths, introduced first by Swenson (ref. 6), use the property that a point in the real supersonic zone can be reached by two characteristics starting at the sonic locus of each characteristic plane (ref. 3). The computation for the supersonic zone is done once the coefficients  $b_n$  in equation (21) have been obtained. So the problem (eq. (18)) is solved only once for these points. This makes the use of a much finer grid for the supersonic computation affordable, both in terms of computing storage and CPU time. The analytic solution is path independent, by the Cauchy Integral theorem, provided that it stays on the proper branch of the solution.

The finite difference scheme

$$\varphi_{i,j} - \varphi_{i-1,j} = \tilde{\tau}_+(\psi_{i,j} - \psi_{i-1,j})$$

$$\varphi_{i,j} - \varphi_{i,j-1} = \tilde{\tau}_-(\psi_{i,j} - \psi_{i,j-1}) \quad (24)$$

is used to integrate the equations. The average values  $\tau_\pm$  are calculated with a predictor-corrector scheme that gives second-order accuracy. A Richardson extrapolation to the zero limit included in the code gives third-order accuracy.

Two complex constants were left at our disposal in the computation of the Riemann functions. To determine them it is required, first, that the stream function be single valued along the airfoil. This leads to the condition for the jump in  $\psi$

$$[\psi] = -2\pi[I_m\{\psi_1(\xi_1, \bar{\xi}_1)\} + I_m\{\psi_2(\xi_2, \bar{\xi}_2)\}] = 0 \quad (25)$$

On the other hand, the circulation  $\Gamma$  over the airfoil is given. This imposes the jump condition on  $\varphi$

$$I_m\{\varphi_1(\xi_1, \bar{\xi}_1)\} - I_m\{\varphi_2(\xi_2, \bar{\xi}_2)\} = \frac{\Gamma}{2\pi} \quad (26)$$

The locations of the stagnation point and trailing edge impose the two remaining conditions needed to determine the four real constants.

With the potential and stream functions completely determined, the body is calculated by using the formula

$$x + iy = \int \frac{e^{i\theta}}{q} \left( d\varphi + \frac{i}{\rho} d\psi \right) \quad (27)$$

From the residuum of this function, when a loop is described around one singularity, say the source  $\xi = \xi_2$ , the repeating vector

$$[x + iy] = -2\pi \frac{e^{i\theta_2}}{q_2} \left[ I_m\{\varphi_2(\xi_2, \bar{\xi}_2)\} + \frac{i}{\rho_2} I_m\{\psi_2(\xi_2, \bar{\xi}_2)\} \right] \quad (28)$$

is obtained. The modulus of this vector is the gap, or distance between adjacent blades. If one considers, instead, a loop which contains both singularities, then the jump in the function  $x + iy$  around the airfoil

$$[x + iy] = -2\pi \left[ \sum_{j=1}^2 \frac{e^{i\theta_j}}{q_j} \left( I_m\{\varphi_j(\xi_j, \bar{\xi}_j)\} + \frac{i}{\rho_j} I_m\{\psi_j(\xi_j, \bar{\xi}_j)\} \right) \right] \quad (29)$$

is obtained. The real and imaginary parts of this vector measures the opening of the airfoil at the trailing edge in the  $x$ - and  $y$ -directions, respectively. This formula can be used to check the accuracy of the computation, when the actual coordinates of the body are obtained.

### Boundary Layer Correction

A turbulent boundary layer computation has been incorporated into the inviscid inverse design code. The lag-entrainment method is followed as developed by Green, Weeks, and Brooman in reference 7. This method contains fewer empirical factors than the classic of Nash and McDonald. It solves three ordinary differential equations (ODE) for three independent parameters, the momentum thickness, the shape factor, and the entrainment coefficient, instead of one ODE for the momentum thickness as in the method of Nash and McDonald.

These three ODE can be written as

$$\frac{d\theta}{ds} = \frac{C_f}{2} - (H + 2 - M^2) \frac{\theta}{q_e} \frac{dq_e}{ds}$$

$$\theta \frac{d\bar{H}}{ds} = \frac{d\bar{H}}{dH_1} \left[ C_E - H_1 \left\{ \frac{C_f}{2} - (H + 1) \frac{\theta}{q_e} \frac{dq_e}{ds} \right\} \right]$$

$$\theta \frac{dC_E}{ds} = F \left[ \frac{2.8}{H + H_1} \left\{ C_{\tau_{EQ}}^{1/2} - \lambda C_{\tau}^{1/2} \right\} + \left( \frac{\theta}{q_e} \frac{dq_e}{ds} \right) EQ - \frac{\theta}{q_e} \frac{dq_e}{ds} \left\{ 1 + f(M^2) \right\} \right] \quad (30)$$

where the three independent parameters  $\theta$ ,  $H$ , and  $C_E$  are defined by

$$\begin{aligned} \theta &= \int_0^\infty \frac{\rho q}{\rho q_e} \left( 1 - \frac{q}{q_e} \right) dy \\ \bar{H} &= \frac{1}{\theta} \int_0^\infty \frac{\rho}{\rho_e q_e} \left( 1 - \frac{q}{q_e} \right) dy \\ C_E &= \frac{1}{\rho_e q_e} \frac{d}{ds} \left( \int_0^\delta \rho q dy \right) \end{aligned} \quad (31)$$

The suffix  $e$  refers to flow variables at the edge of the boundary layer. The two other shape parameters and the skin friction coefficient are defined by

$$\begin{aligned} H &= \frac{\delta^*}{\theta} \\ H_1 &= \frac{1}{\theta} \int_0^\infty \frac{\rho q}{\rho_e q_e} dy \\ C_f &= \frac{\tau_w}{\frac{1}{2} \rho_e q_e^2} \end{aligned} \quad (32)$$

See reference 7 for the definition and value of the other coefficients, which are functions of the entrainment coefficient and the local free-stream magnitudes.

The transition point, at which the computation of the boundary layer is started, is left as an input parameter. Of the three initial values necessary to numerically solve the system of ordinary differential equation (9), only the initial momentum thickness is specified as an input parameter. The other two are computed by means of the equilibrium relations established in reference 7.

As described before, once an inviscid airfoil has been obtained, the turbulent boundary layer correction is switched on. The transition point is usually set at the point where the adverse pressure gradient starts. The Stratford criterion is followed to diffuse the flow from this point to the trailing edge. The Nash-McDonald separation parameter

$$SEP = - \frac{\theta}{q} \frac{dq}{ds} \quad (33)$$

is used to predict separation. Separation is predicted when this parameter reaches a value of 0.004.

To achieve a nonseparated flow, the diffusion part of the input pressure distribution is modified, keeping the circulation constant, until the desired value of the parameter SEP is reached. Each iteration produces a new airfoil with no significant change in the inlet flow conditions and solidity. Instead, the thickness at the trailing edge has to be closely monitored, as it will determine the limits of the process.

## Design Procedure

The design of two-dimensional inviscid subcritical and supercritical cascades has been widely accepted as a method to produce axial compressor and turbine blades. With this method a number of sections, spanning from hub to tip, can be designed independently of each other according to the flow conditions required in the spanwise direction. Five of these two-dimensional sections are usually enough to design a blade with considerable three-dimensional effects.

A wide variety of airfoils in cascade can now be designed with this inverse design procedure. The input to the design code can be separated in three parts. First, a surface speed distribution is specified. The aerodynamic performance on the airfoil is controlled by means of this input speed distribution.

Second, three design parameters must be given. These parameters are the radius  $R$  of the outer circumference of the circular ring in the hodograph domain, which controls the solidity of the cascade; the angle  $\text{THETA}$  which locates the leading edge stagnation point, and thereby controls the stagger angle; and a Mach parameter,  $\text{EMACH}$ , controlling the inlet Mach number.

The third set of parameters, or numerical parameters, is concerned with accuracy versus computational speed of the design process. These parameters are (1) the number of nodes in the exterior circle, equal to the number of Tchebycheff polynomials used in the expansion of the regular part of the solution and (2) the number of iterations, which controls the total number of cycles (each one includes the calculation of the mapping function and a complete solution of the equations). Additionally, two grid sizes can be set, one for the subsonic-transonic computation, and the other, a finer one, for the supersonic computation. A Richardson extrapolation can be included in the last iteration. A complete description of the input parameters is given in appendix A.

To achieve a good design, one could proceed in the following way. An input speed distribution is prescribed that reflects the desired aerodynamic behavior. Then the three design parameters are determined. The parameter  $R$ , that controls the solidity, can be chosen with values that in practical

terms, vary from 1.4 for a solidity of approximately 2 to a value of 2.5 for lower solidities of about 1. In the same manner, the input Mach number EMACH and the angle THETA for the leading edge stagnation point are set.

A run can be made with this set of input parameters, and the design parameters changed successively until the desired inlet flow conditions and solidity are obtained. The advantage of the elliptic transformation is that changes in each of the three parameters have little effect on the flow variables that the two other parameters control. For instance, large changes in the parameter THETA have small effects on the solidity.

Once the required solidity, inlet Mach number, and inlet air angle have been obtained, the input speed distribution is modified. This modification increases or decreases the lift, and thus the turning angle of the blade, by changing the area enclosed by the speed distribution. When the required turning has been achieved, and hence the proper exit flow conditions, the input speed distribution is used to tailor the body geometry. The maximum thickness of the airfoil, the leading edge curvature, and the trailing edge thickness can then be adjusted.

If all the numerical parameters are kept at their default values, a subcritical airfoil can be designed with as little as 30 sec of CPU time per run on the IBM 370-3033 at NASA Lewis. Subcritical designs can be obtained with as few as 15

runs, including the boundary layer correction. This makes the design of subcritical airfoils a very fast and reliable process.

For transonic designs the situation is more complicated. In the first place, it is not known if a shockfree solution exists in the region being searched. The paths of integration, although automated not to intersect the sonic line, can reach a wrong branch of the analytic solution. Also, limit lines can appear in the supersonic region. The number of points in the computational domain is much larger, both because the integration paths are longer and because a finer grid is required, thereby increasing the CPU time considerably. The procedure for a transonic design would be to obtain first a subsonic blade with flow characteristics close to the design in question. Then, by raising the input Mach number a supersonic region will be formed and the design parameters tuned to obtain the desired blade. In the final stages, a transonic run with a fine grid and a Richardson extrapolation in both the subsonic and supersonic regions takes about 5 min of CPU time on the same IBM 370.

Lewis Research Center  
National Aeronautics and Space Administration  
Cleveland, Ohio, November 4, 1986

## Appendix A Input Data

### Description of Input Data Set

The input to the design code is supplied in the data set Fortran Unit Number 2. This data set begins with the input parameters in a NAMELIST form, and is followed by the input speed distribution. This speed distribution is given as a set of points defining speed versus arc length. They are given in

the format X5,2f20.8, which corresponds to the point number, arc length, and speed value. This list is preceded by an integer in format I5, that corresponds to the number of points that follows. An example of an input data set that will reproduce the run corresponding to the supercritical propeller case given in appendix B is as follows:

```
CDATA NRN=1035,R=1.95D0,EMACK=.78D0,THETA=26.0D0,  
NI=3,NF=128,GRID=.06D0,GRIDS=.04D0,IRICH0=1,IRICH1=1,  
RN=1.D+06,TRU=.26D0,TRL=.105D0,RT0=320.DC&END  
27  
1 -.420000 -.924000  
2 -.060000 -.918000  
3 .090000 -.924000  
4 .271800 -.950000  
5 .430000 -.990000  
6 .598000 -1.047000  
7 .755000 -1.132000  
8 .790000 -1.150000  
9 .815000 -1.160000  
10 .835000 -1.163000  
11 .865000 -1.154000  
12 .871000 -1.100000  
13 .888000 0.000000  
14 .904400 1.040000  
15 .910900 1.150000  
16 .920000 1.280000  
17 .940000 1.380000  
18 .980000 1.416000  
19 1.040000 1.441000  
20 1.100000 1.450000  
21 1.146397 1.455000  
22 1.230000 1.461000  
23 1.330000 1.459000  
24 1.460000 1.365000
```

Beside the input data set, three working files, Fortran Unit Numbers 1, 3, and 5 have to be defined. The output file is written in unit number 4, and all the graphics information is stored in Unit Number 7. A separate program will read unit number 7 to produce the plot file corresponding to each run. This graphic subroutine, because of its dependency on a particular machine, will have to be adapted by the users to their particular system.

### Definition of Input Parameters

The input parameters are defined as follows:

NRN	run number
R	radius of outer circle, controls the solidity of the cascade
EMACH	free stream Mach number, controls the inlet Mach number
THETA	angular location of the stagnation point, controls the inlet air angle
NI	number of iterations
NF	number of nodes and Tchebycheff polynomials
GRID	grid size for subsonic and transonic paths
GRIDS	grid size for supersonic paths
IRICHD	a value of 1 or 0 will, respectively, turn on or off a Richardson extrapolation in the last iteration of the flow computation along subsonic and transonic paths
IRICHIS	a value of 1 or 0 will, respectively, turn on or off a Richardson extrapolation in the flow computation along the supersonic paths

RN	reynolds number based on chord; a zero value will skip the boundary layer computation
TRU	x-coordinate where transition is assumed for the suction side
TRL	x-coordinate where transition is assumed for the pressure side
RTHO	reynolds number based on momentum thickness assumed at transition point

When the parameter NI is zero the graphics subroutine produces a spline fit of the input speed distribution. For values of NI greater than zero it gives three other plot frames, as shown in the figures in appendix B.

### Default Values

NRN = 1000
R = 1.50
EMACH = 0.50
THETA = 0.0
NI = 3
NF = 64
GRID = 0.60D-01
GRIDS = 0.40D-01
IRICHD = 0
IRICHIS = 0
RN = 0.0
TRU = 0.20
TRL = 0.20
RTHO = 320.0

## Appendix B Output List

This appendix lists six airfoils designed with the procedure described in the section Design Procedures. The computer output for these six cases are also listed. The first one is a transonic airfoil fit for a midspan section of a modern propeller. An inlet Mach number of 0.83 was reached before the appearance of limiting lines. The maximum thickness to chord ratio of 0.059 is reached at about 45 percent of the chord, which makes it an attractive design. Figure 1(a) shows a hodograph plane for this airfoil. In figure 1(b) can be seen the surface Mach number distribution obtained and the inviscid airfoil. Figure 1(c) shows the relative position of the airfoils in the cascade plane. A cubic spline has been passed through the airfoil after subtracting the computed displacement thickness from the surface of the airfoil in figure 1(b).

The next airfoil, figure 2, represents a tip section for a compressor rotor. The inlet Mach number reached is 0.86. This airfoil shows that after subtraction of the boundary layer the displacement thickness is 0.024. A low speed rotor-tip section with a high inlet air angle of 71° is shown in figure 3.

The code has been used to design two turbine blade sections shown in figures 4 and 5. The first one is a subcritical section with a solidity of 1.77 (gap-to-chord ratio of 0.56). The surface speed distribution presents an accelerated profile on both sides of the blade. A small amount of diffusion is present in the last 30 percent of the suction side to obtain the correct trailing edge opening. This airfoil has been designed to form the midspan section of a cooled turbine rotor.

After this subcritical design, a supercritical turbine blade section is shown with half the solidity of the previous design, and the same flow turning. This, naturally, implies that one-half of the blades are needed for a turbine rotor with this section, with the corresponding savings in weight and fabrication cost. The diffusion on the suction side is now considerably greater, but the reduction in the number of blades allows us to expect higher losses per blade with the same, or less, total loss.

The last example (ref. 8),, shown in figure 6, is a turning vane designed to operate at both zero incidence and at 45° of positive incidence, with the same exit flow angle in both modes of operation. Because of the blunt leading edge, large maximum thickness-to-chord ratio, and high solidity, this blade is capable of turning the flow for the 45° of positive incidence operation mode.

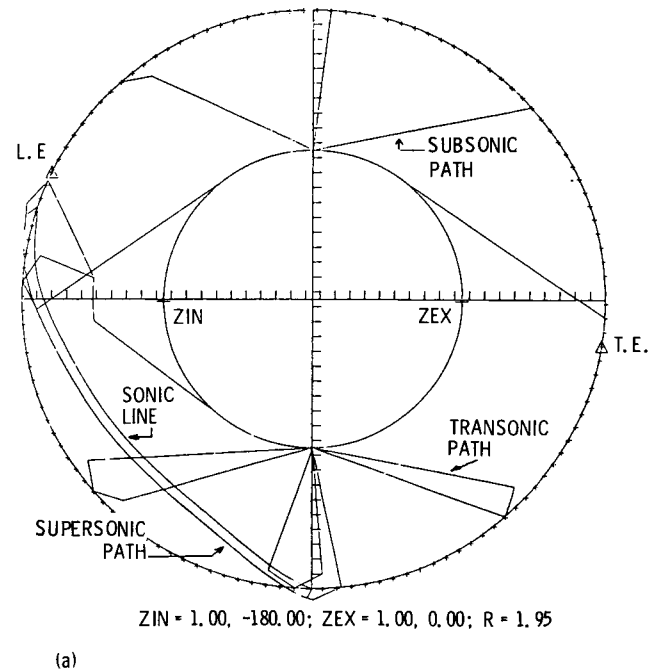
The Mach number distributions in figures 1 and 2 present small spikes near the leading edge, which reflect the beginning of the formation of a limiting line. This is attributable to the high inlet Mach number of both designs. If it is considered that these spikes might trip the boundary layer, they would have to be eliminated by lowering the inlet number.

### Supercritical Propeller

```

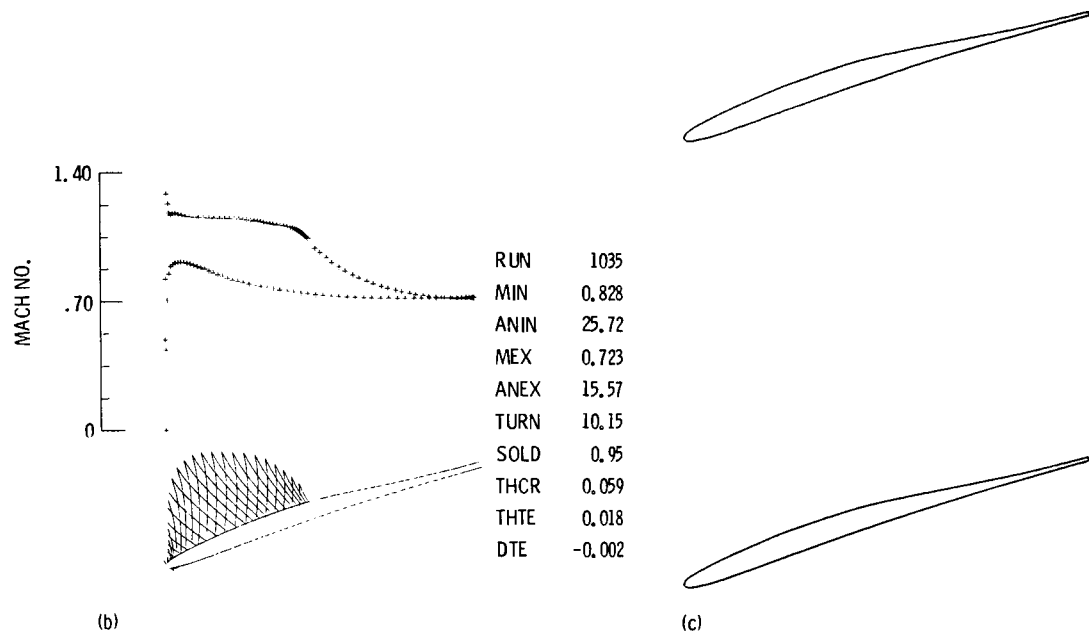
ECDATA
NRN = 1035
R = 1.950
EMACH = 0.780
THETA = 26.0
NI = 3
NF = 128
GRID = 0.80D-01
GRIDS = 0.40D-01
IRICHD = 1
IRICHs = 1
RN = 1000000.0
TRU = 0.260
TRL = 0.1050
RTHO = 320.0
SEND

```



(a) Hodograph plane.

Figure 1.—Supercritical propeller.



(b) Mach number distribution and inviscid airfoil.  
 (c) Relative position of airfoils in cascade plane after boundary layer is subtracted.

Figure 1.—Concluded.

N	ARC	V
1	-0.420000	-0.924000
2	-0.060000	-0.918000
3	0.090000	-0.924000
4	0.271800	-0.950000
5	0.430000	-0.990000
6	0.598000	-1.047000
7	0.755000	-1.132000
8	0.790000	-1.150000
9	0.815000	-1.160000
10	0.835000	-1.163000
11	0.865000	-1.154000
12	0.871000	-1.100000
13	0.888000	0.000000
14	0.904400	1.040000
15	0.910900	1.150000
16	0.920000	1.280000
17	0.940000	1.380000
18	0.980000	1.416000
19	1.040000	1.441000

20	1.100000	1.450000
21	1.146397	1.455000
22	1.280000	1.461000
23	1.330000	1.459000
24	1.460000	1.365000
25	1.610000	1.175500
26	1.900000	0.964000
27	2.182000	0.914000

ITER	MIN	ANIN	TURN	GAP	RESIN
1	0.78	29.20	10.21	1.04	-0.1523D 00
2	0.82	26.50	9.79	1.05	-0.1071D 00
3	0.83	25.72	10.15	1.06	-0.1026D 00

1

INVISCID COMPUTATION

INLET MACH NUMBER = 0.828            INLET FLOW ANGLE = 25.72

EXIT MACH NUMBER = 0.723            EXIT FLOW ANGLE = 15.57

TURNING = 10.145

GAP = 1.058            CHORD = 1.002            AXIAL CHORD = 0.968

GAP/CHORD = 1.055 SOLIDITY = 0.947 AXIAL SOLIDITY = 0.906

THICK/CHORD = 0.059,            DX = -0.0069; DY = 0.0172

THICK/CHORD AT TE = 0.018,            DEV = -0.002

N	X	Y	MACH	ANGL	CURVATURE
1	0.95706	0.21911	0.7115	15.64	0.00
2	0.95706	0.21911	0.7115	15.64	0.00
3	0.95338	0.21808	0.7143	15.55	0.39
4	0.95034	0.21724	0.7139	15.51	0.22

5	0.94080	0.21459	0.7135	15.53	-0.03
6	0.93183	0.21209	0.7129	15.56	-0.05
7	0.91673	0.20788	0.7123	15.60	-0.05
8	0.90243	0.20388	0.7117	15.65	-0.06
9	0.88263	0.19832	0.7110	15.72	-0.06
10	0.86409	0.19309	0.7104	15.80	-0.07
11	0.84079	0.18647	0.7098	15.89	-0.07
12	0.81923	0.18031	0.7093	16.00	-0.08
13	0.79366	0.17295	0.7090	16.12	-0.08
14	0.77025	0.16616	0.7088	16.25	-0.09
15	0.74344	0.15831	0.7087	16.39	-0.09
16	0.71909	0.15111	0.7088	16.54	-0.11
17	0.69182	0.14297	0.7091	16.71	-0.10
18	0.66718	0.13553	0.7096	16.89	-0.12
19	0.64000	0.12722	0.7104	17.09	-0.12
20	0.61550	0.11964	0.7115	17.31	-0.15
21	0.58878	0.11126	0.7131	17.54	-0.14
22	0.56475	0.10360	0.7153	17.78	-0.17
23	0.53875	0.09521	0.7181	18.02	-0.16
24	0.51541	0.08756	0.7215	18.27	-0.17
25	0.49034	0.07923	0.7255	18.50	-0.16
26	0.46783	0.07165	0.7301	18.72	-0.16
27	0.44383	0.06346	0.7352	18.93	-0.14
28	0.42226	0.05602	0.7408	19.12	-0.15
29	0.39940	0.04806	0.7468	19.29	-0.12
30	0.37883	0.04083	0.7531	19.43	-0.11
31	0.35716	0.03315	0.7596	19.56	-0.09
32	0.33760	0.02619	0.7662	19.66	-0.09
33	0.31710	0.01884	0.7728	19.75	-0.07
34	0.29855	0.01217	0.7794	19.83	-0.07
35	0.27922	0.00518	0.7864	19.91	-0.07
36	0.26169	-0.00118	0.7938	19.97	-0.05
37	0.24356	-0.00777	0.8011	19.99	-0.03
38	0.22705	-0.01379	0.8080	20.03	-0.03
39	0.21009	-0.01998	0.8159	20.08	-0.05
40	0.19464	-0.02563	0.8257	20.09	-0.01
41	0.17899	-0.03134	0.8361	20.02	0.08
42	0.16471	-0.03652	0.8459	19.89	0.14
43	0.15038	-0.04169	0.8557	19.73	0.19
44	0.13722	-0.04638	0.8650	19.51	0.27
45	0.12416	-0.05098	0.8739	19.26	0.32
46	0.11208	-0.05516	0.8822	18.95	0.42
47	0.10023	-0.05919	0.8899	18.59	0.50
48	0.08918	-0.06286	0.8966	18.16	0.64
49	0.07849	-0.06632	0.9026	17.66	0.78
50	0.06842	-0.06947	0.9074	17.06	1.00
51	0.05883	-0.07235	0.9110	16.32	1.29
52	0.04970	-0.07495	0.9119	15.40	1.69
53	0.04088	-0.07659	0.9107	14.25	2.24
54	0.03270	-0.07855	0.9071	12.72	3.17
55	0.02525	-0.08010	0.9002	10.55	4.97
56	0.01830	-0.08121	0.8876	7.20	8.32
57	0.01221	-0.08169	0.8486	0.93	17.92

58	0.00672	-0.08128	0.7052	-10.46	36.09
59	0.00197	-0.07965	0.4363	-29.56	66.47
60	-0.00027	-0.07735	0.0001	118.33	174.38
61	-0.00135	-0.07409	0.4919	82.22	183.47
62	0.00097	-0.06836	0.8220	58.77	66.20
63	0.00366	-0.06372	1.2853	44.03	48.02
64	0.00892	-0.05915	1.2339	38.16	14.69
65	0.01280	-0.05627	1.1825	35.12	11.01
66	0.01812	-0.05270	1.1719	32.85	6.17
67	0.02454	-0.04872	1.1793	30.88	4.55
68	0.03266	-0.04401	1.1806	29.48	2.61
69	0.04218	-0.03874	1.1752	28.52	1.54
70	0.05244	-0.03325	1.1693	27.77	1.13
71	0.06399	-0.02726	1.1645	27.11	0.88
72	0.07686	-0.02076	1.1609	26.50	0.73
73	0.09072	-0.01394	1.1583	25.94	0.63
74	0.10581	-0.00668	1.1564	25.40	0.56
75	0.12160	0.00073	1.1551	24.90	0.51
76	0.13798	0.00825	1.1540	24.42	0.47
77	0.15464	0.01573	1.1528	23.96	0.43
78	0.17101	0.02293	1.1515	23.54	0.41
79	0.18712	0.02988	1.1501	23.14	0.40
80	0.20246	0.03638	1.1485	22.75	0.40
81	0.21708	0.04246	1.1469	22.39	0.40
82	0.23096	0.04812	1.1451	22.03	0.41
83	0.24400	0.05335	1.1432	21.69	0.43
84	0.25635	0.05822	1.1410	21.35	0.44
85	0.26788	0.06269	1.1386	21.03	0.46
86	0.27872	0.06683	1.1359	20.71	0.47
87	0.28893	0.07066	1.1329	20.41	0.49
88	0.29865	0.07424	1.1297	20.12	0.50
89	0.30821	0.07772	1.1262	19.82	0.51
90	0.31771	0.08112	1.1227	19.53	0.50
91	0.32718	0.08445	1.1194	19.24	0.50
92	0.33714	0.08790	1.1163	18.95	0.48
93	0.34830	0.09169	1.1130	18.63	0.47
94	0.35969	0.09550	1.1097	18.31	0.47
95	0.37030	0.09898	1.1064	18.00	0.48
96	0.38059	0.10229	1.1027	17.70	0.50
97	0.39006	0.10529	1.0985	17.40	0.53
98	0.39817	0.10781	1.0939	17.12	0.57
99	0.40515	0.10994	1.0890	16.87	0.61
100	0.41112	0.11174	1.0838	16.63	0.66
101	0.41637	0.11329	1.0784	16.41	0.71
102	0.42107	0.11467	1.0729	16.19	0.76
103	0.42536	0.11590	1.0671	15.99	0.80
104	0.42941	0.11706	1.0610	15.79	0.83
105	0.43325	0.11814	1.0549	15.58	0.89
106	0.43693	0.11915	1.0495	15.37	0.96
107	0.44062	0.12016	1.0439	15.16	0.95
108	0.44438	0.12117	1.0371	14.96	0.92
109	0.46644	0.12681	0.9820	13.98	0.75
110	0.48139	0.13039	0.9579	13.37	0.69

111	0.50150	0.13507	0.9289	12.82	0.47
112	0.51844	0.13885	0.9022	12.39	0.43
113	0.54079	0.14370	0.8781	12.06	0.25
114	0.55887	0.14751	0.8563	11.82	0.23
115	0.58243	0.15241	0.8363	11.66	0.12
116	0.60127	0.15628	0.8183	11.58	0.07
117	0.62557	0.16126	0.8020	11.56	0.01
118	0.64489	0.16521	0.7874	11.61	-0.04
119	0.66952	0.17029	0.7744	11.70	-0.06
120	0.68902	0.17435	0.7628	11.84	-0.12
121	0.71362	0.17955	0.7525	12.01	-0.12
122	0.73299	0.18370	0.7435	12.21	-0.18
123	0.75716	0.18898	0.7355	12.43	-0.16
124	0.77601	0.19317	0.7286	12.68	-0.22
125	0.79930	0.19847	0.7227	12.94	-0.19
126	0.81716	0.20262	0.7178	13.21	-0.26
127	0.83902	0.20781	0.7140	13.49	-0.21
128	0.85531	0.21175	0.7109	13.76	-0.28
129	0.87508	0.21664	0.7087	14.02	-0.22
130	0.88907	0.22017	0.7072	14.27	-0.30
131	0.90597	0.22450	0.7063	14.50	-0.23
132	0.91685	0.22734	0.7058	14.71	-0.33
133	0.92999	0.23081	0.7056	14.90	-0.25
134	0.93684	0.23265	0.7057	15.09	-0.46
135	0.94529	0.23494	0.7059	15.26	-0.35
136	0.94721	0.23546	0.7070	15.50	-2.11
137	0.95014	0.23628	0.7115	15.64	-0.79

1

#### BOUNDARY LAYER CORRECTION

#### PRESSURE SIDE

N	X	Y	EM	TH	SEP
60	-0.00027	-0.07735	0.00010		
59	0.00197	-0.07965	0.43634		
58	0.00672	-0.08128	0.70516		
57	0.01221	-0.08169	0.84861		
56	0.01830	-0.08121	0.88759		
55	0.02525	-0.08010	0.90024		
54	0.03270	-0.07855	0.90708		
53	0.04088	-0.07659	0.91065		
52	0.04970	-0.07495	0.91189		
51	0.05863	-0.07235	0.91098		
50	0.06842	-0.06947	0.90742		
49	0.07849	-0.06632	0.90261		
48	0.08918	-0.06286	0.89658		
47	0.10023	-0.05919	0.88985		
46	0.11208	-0.05516	0.88217	0.00030	0.00007

45	0.12416	-0.05098	0.87392	0.00035	0.00024
44	0.13722	-0.04638	0.86497	0.00039	0.00027
43	0.15038	-0.04169	0.85566	0.00043	0.00031
42	0.16471	-0.03652	0.84592	0.00048	0.00034
41	0.17899	-0.03134	0.83614	0.00053	0.00037
40	0.19464	-0.02563	0.82572	0.00059	0.00040
39	0.21009	-0.01998	0.81593	0.00064	0.00037
38	0.22705	-0.01379	0.80803	0.00070	0.00033
37	0.24356	-0.00777	0.80106	0.00075	0.00033
36	0.26169	-0.00118	0.79384	0.00081	0.00036
35	0.27922	0.00518	0.78638	0.00087	0.00038
34	0.29855	0.01217	0.77935	0.00093	0.00037
33	0.31710	0.01884	0.77276	0.00099	0.00038
32	0.33760	0.02619	0.76618	0.00106	0.00039
31	0.35716	0.03315	0.75965	0.00112	0.00041
30	0.37883	0.04083	0.75314	0.00119	0.00042
29	0.39940	0.04806	0.74684	0.00126	0.00042
28	0.42226	0.05602	0.74079	0.00133	0.00041
27	0.44383	0.06346	0.73519	0.00140	0.00039
26	0.46783	0.07165	0.73006	0.00147	0.00037
25	0.49034	0.07923	0.72551	0.00154	0.00034
24	0.51541	0.08756	0.72150	0.00161	0.00030
23	0.53875	0.09521	0.71812	0.00167	0.00026
22	0.56475	0.10360	0.71531	0.00173	0.00021
21	0.58878	0.11126	0.71314	0.00179	0.00017
20	0.61550	0.11964	0.71151	0.00185	0.00012
19	0.64000	0.12722	0.71038	0.00190	0.00009
18	0.66718	0.13553	0.70961	0.00196	0.00006
17	0.69182	0.14297	0.70913	0.00201	0.00004
16	0.71909	0.15111	0.70883	0.00206	0.00002
15	0.74344	0.15831	0.70871	0.00210	0.00000
14	0.77025	0.16616	0.70875	0.00215	-0.00001
13	0.79366	0.17295	0.70897	0.00219	-0.00003
12	0.81923	0.18031	0.70931	0.00223	-0.00005
11	0.84079	0.18647	0.70979	0.00227	-0.00007
10	0.86409	0.19309	0.71036	0.00230	-0.00009
9	0.88263	0.19832	0.71101	0.00233	-0.00010
8	0.90243	0.20388	0.71167	0.00236	-0.00012
7	0.91673	0.20788	0.71235	0.00238	-0.00013
6	0.93183	0.21209	0.71294	0.00240	-0.00016
5	0.94080	0.21459	0.71351	0.00241	-0.00015
4	0.95034	0.21724	0.71386	0.00243	-0.00034
3	0.95338	0.21808	0.71428	0.00243	0.00079
2	0.95706	0.21911	0.71153	0.00246	0.00225
1	0.95706	0.21911	0.71153	0.00246	0.00225

## SUCTION SIDE

N	X	Y	EM	TH	SEP
61	-0.00135	-0.07409	0.49186		
62	0.00097	-0.06836	0.82204		
63	0.00366	-0.06372	1.28531		
64	0.00892	-0.05915	1.23395		
65	0.01280	-0.05627	1.18254		
66	0.01812	-0.05270	1.17191		
67	0.02454	-0.04872	1.17926		
68	0.03266	-0.04401	1.18063		
69	0.04218	-0.03874	1.17519		
70	0.05244	-0.03325	1.16929		
71	0.06399	-0.02726	1.16455		
72	0.07686	-0.02076	1.16090		
73	0.09072	-0.01394	1.15828		
74	0.10581	-0.00668	1.15642		
75	0.12160	0.00073	1.15509		
76	0.13798	0.00825	1.15397		
77	0.15464	0.01573	1.15280		
78	0.17101	0.02293	1.15150		
79	0.18712	0.02988	1.15005		
80	0.20246	0.03638	1.14851		
81	0.21708	0.04246	1.14687		
82	0.23096	0.04812	1.14509		
83	0.24400	0.05335	1.14316		
84	0.25635	0.05822	1.14099		
85	0.26788	0.06269	1.13859	0.00028	0.00006
86	0.27872	0.06683	1.13590	0.00032	0.00006
87	0.28893	0.07066	1.13292	0.00034	0.00007
88	0.29865	0.07424	1.12969	0.00037	0.00009
89	0.30821	0.07772	1.12623	0.00040	0.00010
90	0.31771	0.08112	1.12273	0.00042	0.00010
91	0.32718	0.08445	1.11943	0.00045	0.00010
92	0.33714	0.08790	1.11626	0.00048	0.00010
93	0.34830	0.09169	1.11297	0.00051	0.00010
94	0.35969	0.09550	1.10967	0.00053	0.00011
95	0.37030	0.09898	1.10639	0.00056	0.00013
96	0.38059	0.10229	1.10270	0.00059	0.00017
97	0.39006	0.10529	1.09847	0.00061	0.00022
98	0.39817	0.10781	1.09390	0.00064	0.00029
99	0.40515	0.10994	1.08897	0.00066	0.00038
100	0.41112	0.11174	1.08383	0.00068	0.00047
101	0.41637	0.11329	1.07843	0.00070	0.00057
102	0.42107	0.11467	1.07286	0.00071	0.00067
103	0.42536	0.11590	1.06706	0.00073	0.00078
104	0.42941	0.11706	1.06096	0.00075	0.00087
105	0.43325	0.11814	1.05492	0.00077	0.00088
106	0.43693	0.11915	1.04955	0.00078	0.00090
107	0.44062	0.12016	1.04385	0.00080	0.00103
108	0.44438	0.12117	1.03713	0.00082	0.00124
109	0.46644	0.12681	0.98203	0.00097	0.00164

110	0.48139	0.13039	0.95786	0.00106	0.00146
111	0.50150	0.13507	0.92886	0.00117	0.00169
112	0.51844	0.13885	0.90215	0.00129	0.00168
113	0.54079	0.14370	0.87812	0.00142	0.00165
114	0.55887	0.14751	0.85632	0.00154	0.00165
115	0.58243	0.15241	0.83633	0.00167	0.00163
116	0.60127	0.15628	0.81831	0.00180	0.00162
117	0.62557	0.16126	0.80201	0.00194	0.00156
118	0.64489	0.16521	0.78743	0.00206	0.00152
119	0.66952	0.17029	0.77440	0.00219	0.00145
120	0.68902	0.17435	0.76281	0.00231	0.00139
121	0.71362	0.17955	0.75254	0.00244	0.00130
122	0.73299	0.18370	0.74345	0.00255	0.00124
123	0.75716	0.18898	0.73548	0.00266	0.00114
124	0.77601	0.19317	0.72857	0.00275	0.00106
125	0.79930	0.19847	0.72271	0.00285	0.00093
126	0.81716	0.20262	0.71784	0.00293	0.00083
127	0.83902	0.20781	0.71395	0.00300	0.00068
128	0.85531	0.21175	0.71093	0.00306	0.00058
129	0.87508	0.21664	0.70872	0.00311	0.00043
130	0.88907	0.22017	0.70720	0.00315	0.00033
131	0.90597	0.22450	0.70627	0.00318	0.00019
132	0.91685	0.22734	0.70579	0.00320	0.00012
133	0.92999	0.23081	0.70561	0.00322	-0.00003
134	0.93684	0.23265	0.70573	0.00323	-0.00007
135	0.94529	0.23494	0.70587	0.00324	-0.00191
136	0.94721	0.23546	0.70699	0.00323	-0.00232
137	0.95014	0.23628	0.71153	0.00321	-0.00230

#### BODY COORDINATES AFTER BOUNDARY LAYER SUBTRACTION

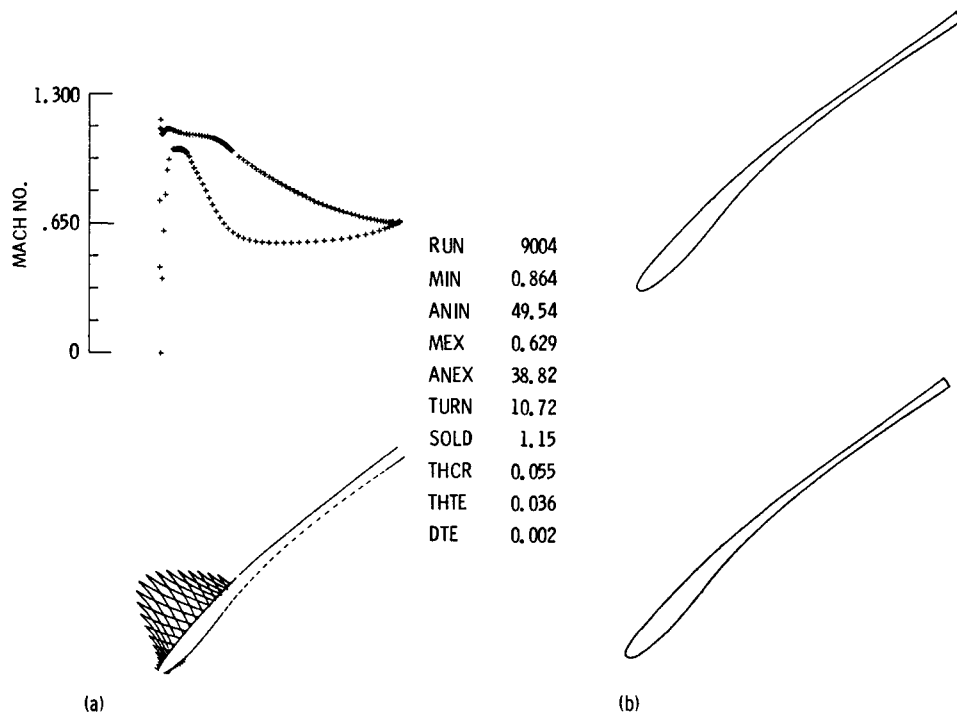
N	XV	Y	N	XV	Y
1	0.95600	0.22291	17	0.69085	0.14622
2	0.95600	0.22291	18	0.66622	0.13871
3	0.95232	0.22187	19	0.63904	0.13034
4	0.94930	0.22098	20	0.61456	0.12268
5	0.93976	0.21833	21	0.58784	0.11422
6	0.93079	0.21582	22	0.56382	0.10649
7	0.91569	0.21159	23	0.53784	0.09801
8	0.90140	0.20757	24	0.51451	0.09026
9	0.88160	0.20198	25	0.48947	0.08184
10	0.86306	0.19671	26	0.46698	0.07416
11	0.83977	0.19005	27	0.44300	0.06587
12	0.81822	0.18384	28	0.42147	0.05832
13	0.79265	0.17644	29	0.39864	0.05025
14	0.76925	0.16958	30	0.37810	0.04291
15	0.74245	0.16168	31	0.35646	0.03513
16	0.71811	0.15442	32	0.33694	0.02805
			33	0.31647	0.02061
			34	0.29795	0.01383
			35	0.27865	0.00675

N	XV	Y	N	XV	Y
36	0.26116	0.00029	90	0.31803	0.08021
37	0.24306	-0.00639	91	0.32751	0.08349
38	0.22657	-0.01249	92	0.33748	0.08688
39	0.20964	-0.01876	93	0.34866	0.09063
40	0.19423	-0.02449	94	0.36006	0.09438
41	0.17861	-0.03029	95	0.37068	0.09781
42	0.16437	-0.03556	96	0.38098	0.10108
43	0.15006	-0.04081	97	0.39046	0.10403
44	0.13694	-0.04558	98	0.39857	0.10650
45	0.12391	-0.05027	99	0.40555	0.10860
46	0.11189	-0.05461	100	0.41153	0.11036
47	0.10023	-0.05919	101	0.41678	0.11188
48	0.08918	-0.06286	102	0.42150	0.11322
49	0.07849	-0.06632	103	0.42578	0.11442
50	0.06842	-0.06947	104	0.42984	0.11553
51	0.05883	-0.07235	105	0.43368	0.11657
52	0.04970	-0.07495	106	0.43737	0.11755
53	0.04088	-0.07659	107	0.44107	0.11852
54	0.03270	-0.07855	108	0.44490	0.11923
55	0.02525	-0.08010	109	0.46698	0.12465
56	0.01830	-0.08121	110	0.48197	0.12796
57	0.01221	-0.08169	111	0.50212	0.13238
58	0.00672	-0.08128	112	0.51909	0.13588
59	0.00197	-0.07965	113	0.54148	0.14049
60	-0.00027	-0.07735	114	0.55959	0.14405
61	-0.00135	-0.07409	115	0.58319	0.14874
62	0.00097	-0.06836	116	0.60207	0.15238
63	0.00366	-0.06372	117	0.62640	0.15717
64	0.00892	-0.05915	118	0.64577	0.16092
65	0.01280	-0.05627	119	0.67044	0.16584
66	0.01812	-0.05270	120	0.69000	0.16972
67	0.02454	-0.04872	121	0.71464	0.17478
68	0.03266	-0.04401	122	0.73405	0.17878
69	0.04218	-0.03874	123	0.75827	0.18395
70	0.05244	-0.03325	124	0.77717	0.18803
71	0.06399	-0.02726	125	0.80050	0.19325
72	0.07686	-0.02076	126	0.81840	0.19732
73	0.09072	-0.01394	127	0.84030	0.20247
74	0.10581	-0.00668	128	0.85662	0.20638
75	0.12160	0.00073	129	0.87642	0.21126
76	0.13798	0.00825	130	0.89045	0.21478
77	0.15464	0.01573	131	0.90736	0.21913
78	0.17101	0.02293	132	0.91826	0.22197
79	0.18712	0.02988	133	0.93141	0.22547
80	0.20246	0.03638	134	0.93828	0.22731
81	0.21708	0.04246	135	0.94673	0.22966
82	0.23096	0.04812	136	0.94866	0.23023
83	0.24400	0.05335	137	0.95160	0.23105
84	0.25635	0.05822			
85	0.26811	0.06212			
86	0.27899	0.06612			
87	0.28921	0.06990			
88	0.29894	0.07344			
89	0.30851	0.07686			

DXV = -0.0044; DYV = 0.0081

THICK/CHORD AT TE 0.009, DEV = -0.002

## Supercritical Rotor Blade



(a) Mach number distribution and inviscid airfoil.  
 (b) Relative position of airfoils in cascade plane after boundary layer is subtracted.

Figure 2.—Supercritical rotor.

	N	ARC	V
QDATA	1	-0.176000	-0.940000
NRN= 9004	2	-0.060000	-0.870000
R= 1.80	3	0.090000	-0.820000
EMACH= 0.720	4	0.274800	-0.795000
THETA= 39.3750	5	0.480000	-0.812000
NI= 3	6	0.600000	-0.925000
NF= 128	7	0.755000	-1.290000
GRID= 0.60D-01	8	0.855000	-1.295000
GRIDS= 0.30D-01	9	0.870000	-1.060000
IRICHd= 1	10	0.885000	0.000000
IRICHs= 1	11	0.900700	1.350000
RN= 1000000.0	12	0.904000	1.379000
TRU= 0.50D-01	13	0.917000	1.415000
TRL= 0.80D-01	14	0.926500	1.438000
RTHO= 320.0	15	0.944500	1.470000
QEND	16	0.962000	1.485000
1	17	0.984000	1.490000
	18	1.010000	1.490000
	19	1.050000	1.490000
	20	1.080000	1.490000
	21	1.126397	1.481000
	22	1.320000	1.335000
	23	1.610000	1.090000

24        1.935000        0.930000

ITER	MIN	ANIN	TURN	GAP	RESID
1	0.82	54.62	12.44	0.89	-0.1305D 00
2	0.85	51.73	11.30	0.87	-0.5617D-01
3	0.86	49.54	10.72	0.87	-0.3543D-01

1

INVISCID COMPUTATION

INLET MACH NUMBER = 0.834            INLET FLOW ANGLE = 49.54  
EXIT MACH NUMBER = 0.629            EXIT FLOW ANGLE = 38.82  
                        TURNING = 10.721  
GAP = 0.870            CHORD = 0.999            AXIAL CHORD = 0.744  
GAP/CHORD = 0.871    SOLIDITY = 1.148    AXIAL SOLIDITY = 0.854  
THICK/CHORD = 0.055,        DX = -0.0206; DY = 0.0297  
THICK/CHORD AT TE = 0.036,        DEV = 0.002

N	X	Y	MACH	ANGL	CURVATURE
1	0.76191	0.64890	0.6712	38.07	0.00
2	0.76184	0.64885	0.6713	37.99	17.49
3	0.76057	0.64786	0.6688	37.56	4.62
4	0.75687	0.64505	0.6649	37.14	1.57
5	0.75084	0.64051	0.6593	36.74	0.92
6	0.74200	0.63396	0.6523	36.39	0.56
7	0.73050	0.62553	0.6440	36.11	0.35
8	0.71607	0.61504	0.6347	35.92	0.18
9	0.69901	0.60271	0.6248	35.84	0.06
10	0.67930	0.58847	0.6149	35.90	-0.04

11	0.65748	0.57262	0.6054	36.09	-0.12
12	0.63375	0.55523	0.5967	36.39	-0.18
13	0.60876	0.53667	0.5889	36.80	-0.23
14	0.58279	0.51707	0.5823	37.30	-0.26
15	0.55642	0.49679	0.5768	37.85	-0.29
16	0.52990	0.47596	0.5723	38.45	-0.31
17	0.50363	0.45487	0.5686	39.08	-0.33
18	0.47775	0.43360	0.5656	39.74	-0.34
19	0.45247	0.41232	0.5631	40.44	-0.37
20	0.42786	0.39108	0.5609	41.19	-0.40
21	0.40403	0.36992	0.5593	42.02	-0.45
22	0.38102	0.34886	0.5586	42.94	-0.52
23	0.35891	0.32793	0.5593	43.94	-0.58
24	0.33776	0.30717	0.5617	45.01	-0.63
25	0.31760	0.28661	0.5660	46.13	-0.67
26	0.29848	0.26633	0.5726	47.26	-0.71
27	0.28038	0.24635	0.5815	48.39	-0.73
28	0.26337	0.22682	0.5936	49.51	-0.75
29	0.24739	0.20775	0.6095	50.55	-0.73
30	0.23251	0.18937	0.6299	51.44	-0.65
31	0.21859	0.17170	0.6549	52.08	-0.50
32	0.20567	0.15499	0.6842	52.41	-0.27
33	0.19354	0.13923	0.7166	52.39	0.02
34	0.18219	0.12457	0.7505	52.06	0.31
35	0.17143	0.11090	0.7849	51.49	0.58
36	0.16128	0.09831	0.8187	50.72	0.82
37	0.15160	0.08665	0.8511	49.84	1.02
38	0.14243	0.07596	0.8815	48.87	1.19
39	0.13367	0.06610	0.9080	47.89	1.31
40	0.12533	0.05702	0.9325	46.97	1.29
41	0.11749	0.04876	0.9617	46.03	1.44
42	0.11025	0.04149	0.9890	45.00	1.76
43	0.10265	0.03393	1.0094	43.87	1.85
44	0.09926	0.03070	1.0135	43.38	1.82
45	0.09592	0.02757	1.0167	42.91	1.80
46	0.09255	0.02447	1.0209	42.43	1.83
47	0.08928	0.02151	1.0238	41.96	1.86
48	0.08613	0.01870	1.0253	41.49	1.92
49	0.08302	0.01596	1.0269	41.02	2.01
50	0.07997	0.01334	1.0280	40.53	2.11
51	0.07705	0.01086	1.0276	40.04	2.24
52	0.07418	0.00847	1.0269	39.52	2.40
53	0.07133	0.00614	1.0261	38.98	2.59
54	0.06855	0.00391	1.0242	38.41	2.80
55	0.06574	0.00172	1.0238	37.76	3.16
56	0.06291	-0.00045	1.0266	37.00	3.72
57	0.06027	-0.00241	1.0250	36.20	4.26
58	0.04823	-0.01118	0.9742	30.10	7.14
59	0.04256	-0.01422	0.9201	25.12	13.50
60	0.03730	-0.01627	0.7978	17.17	24.61
61	0.03137	-0.01758	0.6151	6.73	29.98
62	0.02669	-0.01749	0.3771	-9.67	61.26
63	0.02222	-0.01551	0.0001	141.70	102.02

64	0.01885	-0.01144	0.4337	109.65	105.77
65	0.01825	-0.00634	0.7689	86.45	78.97
66	0.01973	-0.00105	1.1313	71.46	47.58
67	0.02165	0.00355	1.1741	64.81	23.28
68	0.02315	0.00655	1.1256	62.06	14.29
69	0.02489	0.00969	1.1038	60.09	9.56
70	0.02738	0.01386	1.1008	58.44	5.93
71	0.03038	0.01861	1.1085	56.92	4.75
72	0.03406	0.02410	1.1183	55.58	3.51
73	0.03844	0.03036	1.1266	54.46	2.56
74	0.04332	0.03707	1.1295	53.58	1.87
75	0.04870	0.04427	1.1283	52.86	1.38
76	0.05473	0.05214	1.1251	52.27	1.05
77	0.06142	0.06070	1.1210	51.76	0.83
78	0.06870	0.06986	1.1168	51.30	0.68
79	0.07653	0.07956	1.1128	50.89	0.58
80	0.08484	0.08972	1.1092	50.51	0.50
81	0.09355	0.10022	1.1062	50.16	0.45
82	0.10259	0.11100	1.1036	49.84	0.41
83	0.11191	0.12198	1.1015	49.52	0.38
84	0.12139	0.13302	1.0998	49.22	0.36
85	0.13092	0.14401	1.0982	48.93	0.35
86	0.14043	0.15487	1.0967	48.65	0.34
87	0.14974	0.16540	1.0950	48.37	0.35
88	0.15865	0.17537	1.0931	48.10	0.35
89	0.16699	0.18463	1.0908	47.83	0.37
90	0.17464	0.19304	1.0882	47.58	0.39
91	0.18152	0.20053	1.0852	47.34	0.42
92	0.18770	0.20721	1.0820	47.10	0.45
93	0.19329	0.21320	1.0786	46.88	0.48
94	0.19839	0.21863	1.0749	46.66	0.50
95	0.20313	0.22364	1.0709	46.46	0.52
96	0.20763	0.22835	1.0666	46.26	0.52
97	0.21198	0.23288	1.0620	46.07	0.52
98	0.21628	0.23734	1.0574	45.89	0.52
99	0.22059	0.24176	1.0528	45.70	0.52
100	0.22463	0.24589	1.0480	45.52	0.55
101	0.22807	0.24938	1.0426	45.34	0.63
102	0.23121	0.25255	1.0368	45.17	0.68
103	0.23489	0.25625	1.0313	44.99	0.61
104	0.23928	0.26061	1.0263	44.79	0.54
105	0.24355	0.26484	1.0208	44.60	0.56
106	0.26514	0.28568	0.9902	43.65	0.55
107	0.27903	0.29887	0.9752	43.13	0.48
108	0.29191	0.31080	0.9598	42.62	0.51
109	0.30587	0.32354	0.9447	42.14	0.44
110	0.31889	0.33522	0.9301	41.69	0.45
111	0.33265	0.34739	0.9161	41.28	0.39
112	0.34554	0.35863	0.9025	40.90	0.39
113	0.35904	0.37025	0.8895	40.55	0.34
114	0.37177	0.38108	0.8769	40.24	0.33
115	0.38505	0.39226	0.8648	39.96	0.28
116	0.39762	0.40275	0.8531	39.72	0.26

117	0.41073	0.41359	0.8418	39.50	0.22
118	0.42321	0.42385	0.8309	39.31	0.20
119	0.43620	0.43446	0.8204	39.15	0.17
120	0.44864	0.44456	0.8104	39.02	0.14
121	0.46156	0.45501	0.8014	38.91	0.12
122	0.47398	0.46501	0.7925	38.76	0.17
123	0.48691	0.47536	0.7814	38.62	0.14
124	0.49944	0.48537	0.7708	38.62	-0.00
125	0.51243	0.49575	0.7629	38.64	-0.02
126	0.52499	0.50579	0.7554	38.61	0.03
127	0.53797	0.51614	0.7476	38.59	0.02
128	0.55055	0.52618	0.7401	38.57	0.01
129	0.56351	0.53652	0.7329	38.57	0.00
130	0.57609	0.54655	0.7261	38.58	-0.00
131	0.58897	0.55683	0.7196	38.58	-0.01
132	0.60145	0.56678	0.7134	38.60	-0.01
133	0.61415	0.57693	0.7075	38.61	-0.01
134	0.62640	0.58671	0.7020	38.62	-0.02
135	0.63878	0.59660	0.6969	38.64	-0.02
136	0.65062	0.60606	0.6921	38.65	-0.02
137	0.66245	0.61553	0.6877	38.66	-0.01
138	0.67363	0.62448	0.6836	38.67	-0.01
139	0.68463	0.63328	0.6799	38.68	-0.01
140	0.69482	0.64144	0.6766	38.68	-0.00
141	0.70460	0.64927	0.6737	38.68	0.00
142	0.71337	0.65630	0.6712	38.68	0.01
143	0.72144	0.66275	0.6692	38.67	0.02
144	0.72822	0.66818	0.6678	38.64	0.05
145	0.73395	0.67275	0.6664	38.61	0.07
146	0.73804	0.67602	0.6671	38.63	-0.07
147	0.74066	0.67811	0.6707	38.43	1.05
148	0.74134	0.67865	0.6712	38.07	7.37

1

#### BOUNDARY LAYER CORRECTION

#### PRESSURE SIDE

N	X	Y	EM	TH	SEP
63	0.02222	-0.01551	0.00009		
62	0.02669	-0.01749	0.37708		
61	0.03137	-0.01758	0.61508		
60	0.03730	-0.01627	0.79784		
59	0.04256	-0.01422	0.92009		
58	0.04823	-0.01118	0.97422		
57	0.06027	-0.00241	1.02504		
56	0.06291	-0.00045	1.02661		
55	0.06574	0.00172	1.02382		
54	0.06855	0.00391	1.02425		

53	0.07133	0.00614	1.02608		
52	0.07418	0.00847	1.02687		
51	0.07705	0.01086	1.02760		
50	0.07997	0.01334	1.02798		
49	0.08302	0.01596	1.02692	0.00028	0.00006
48	0.08613	0.01870	1.02530	0.00029	0.00009
47	0.08928	0.02151	1.02381	0.00031	0.00013
46	0.09255	0.02447	1.02088	0.00032	0.00021
45	0.09592	0.02757	1.01666	0.00033	0.00022
44	0.09926	0.03070	1.01351	0.00035	0.00023
43	0.10265	0.03393	1.00943	0.00036	0.00038
42	0.11025	0.04149	0.98904	0.00041	0.00086
41	0.11749	0.04876	0.96167	0.00046	0.00112
40	0.12533	0.05702	0.93252	0.00052	0.00113
39	0.13367	0.06610	0.90800	0.00058	0.00116
38	0.14243	0.07596	0.88146	0.00065	0.00142
37	0.15160	0.08665	0.85108	0.00074	0.00174
36	0.16128	0.09831	0.81871	0.00084	0.00207
35	0.17143	0.11090	0.78487	0.00097	0.00242
34	0.18219	0.12457	0.75055	0.00113	0.00278
33	0.19354	0.13923	0.71657	0.00132	0.00311
32	0.20567	0.15499	0.68417	0.00154	0.00333
31	0.21859	0.17170	0.65487	0.00179	0.00335
30	0.23251	0.18937	0.62988	0.00205	0.00314
29	0.24739	0.20775	0.60953	0.00231	0.00276
28	0.26337	0.22682	0.59361	0.00255	0.00229
27	0.28038	0.24635	0.58154	0.00275	0.00182
26	0.29848	0.26633	0.57258	0.00292	0.00139
25	0.31760	0.28661	0.56604	0.00306	0.00100
24	0.33776	0.30717	0.56169	0.00317	0.00062
23	0.35891	0.32793	0.55929	0.00325	0.00028
22	0.38102	0.34886	0.55862	0.00329	0.00000
21	0.40403	0.36992	0.55931	0.00332	-0.00020
20	0.42786	0.39108	0.56094	0.00333	-0.00033
19	0.45247	0.41232	0.56309	0.00334	-0.00040
18	0.47775	0.43360	0.56563	0.00335	-0.00046
17	0.50363	0.45487	0.56863	0.00335	-0.00055
16	0.52990	0.47596	0.57231	0.00334	-0.00066
15	0.55642	0.49679	0.57682	0.00332	-0.00080
14	0.58279	0.51707	0.58234	0.00329	-0.00097
13	0.60876	0.53667	0.58895	0.00324	-0.00115
12	0.63375	0.55523	0.59668	0.00317	-0.00134
11	0.65748	0.57262	0.60540	0.00310	-0.00153
10	0.67930	0.58847	0.61492	0.00302	-0.00171
9	0.69901	0.60271	0.62482	0.00293	-0.00188
8	0.71607	0.61504	0.63469	0.00284	-0.00203
7	0.73050	0.62553	0.64398	0.00277	-0.00218
6	0.74200	0.63396	0.65233	0.00270	-0.00232
5	0.75084	0.64051	0.65934	0.00265	-0.00255
4	0.75687	0.64505	0.66491	0.00260	-0.00283
3	0.76057	0.64786	0.66876	0.00257	-0.00482
2	0.76184	0.64885	0.67128	0.00255	-0.00547
1	0.76191	0.64890	0.67117	0.00255	-0.00547

## SUCTION SIDE

N	X	Y	EM	TH	SEP
64	0.01885	-0.01144	0.43371		
65	0.01825	-0.00634	0.76891		
66	0.01973	-0.00105	1.13127		
67	0.02165	0.00355	1.17414		
68	0.02315	0.00655	1.12562		
69	0.02489	0.00969	1.10375		
70	0.02738	0.01386	1.10076		
71	0.03038	0.01861	1.10850		
72	0.03406	0.02410	1.11831		
73	0.03844	0.03036	1.12656		
74	0.04332	0.03707	1.12950		
75	0.04870	0.04427	1.12829		
76	0.05473	0.05214	1.12507	0.00028	0.00006
77	0.06142	0.06070	1.12102	0.00031	0.00008
78	0.06870	0.06986	1.11681	0.00034	0.00009
79	0.07653	0.07956	1.11282	0.00037	0.00008
80	0.08484	0.08972	1.10925	0.00041	0.00008
81	0.09355	0.10022	1.10619	0.00044	0.00007
82	0.10259	0.11100	1.10364	0.00047	0.00006
83	0.11191	0.12198	1.10154	0.00051	0.00005
84	0.12139	0.13302	1.09977	0.00054	0.00005
85	0.13092	0.14401	1.09820	0.00058	0.00005
86	0.14043	0.15487	1.09668	0.00061	0.00005
87	0.14974	0.16540	1.09504	0.00064	0.00006
88	0.15865	0.17537	1.09313	0.00067	0.00008
89	0.16699	0.18463	1.09084	0.00070	0.00011
90	0.17464	0.19304	1.08818	0.00072	0.00015
91	0.18152	0.20053	1.08520	0.00075	0.00018
92	0.18770	0.20721	1.08203	0.00077	0.00023
93	0.19329	0.21320	1.07862	0.00079	0.00028
94	0.19839	0.21863	1.07495	0.00081	0.00034
95	0.20313	0.22364	1.07092	0.00083	0.00040
96	0.20763	0.22835	1.06661	0.00085	0.00046
97	0.21198	0.23288	1.06202	0.00087	0.00050
98	0.21628	0.23734	1.05740	0.00089	0.00052
99	0.22059	0.24176	1.05282	0.00091	0.00057
100	0.22463	0.24589	1.04804	0.00093	0.00072
101	0.22807	0.24938	1.04264	0.00095	0.00092
102	0.23121	0.25255	1.03677	0.00097	0.00093
103	0.23489	0.25625	1.03128	0.00100	0.00075
104	0.23928	0.26061	1.02628	0.00102	0.00071
105	0.24355	0.26484	1.02081	0.00104	0.00080
106	0.26514	0.28568	0.99023	0.00117	0.00089
107	0.27903	0.29887	0.97522	0.00124	0.00092
108	0.29191	0.31080	0.95979	0.00132	0.00100
109	0.30587	0.32354	0.94470	0.00140	0.00106

110	0.31889	0.33522	0.93012	0.00148	0.00111
111	0.33265	0.34739	0.91605	0.00156	0.00117
112	0.34554	0.35863	0.90253	0.00165	0.00123
113	0.35904	0.37025	0.88949	0.00174	0.00128
114	0.37177	0.38108	0.87695	0.00183	0.00134
115	0.38505	0.39226	0.86483	0.00192	0.00140
116	0.39762	0.40275	0.85314	0.00201	0.00145
117	0.41073	0.41359	0.84184	0.00211	0.00150
118	0.42321	0.42385	0.83092	0.00220	0.00155
119	0.43620	0.43446	0.82043	0.00230	0.00158
120	0.44864	0.44456	0.81038	0.00240	0.00156
121	0.46156	0.45501	0.80138	0.00250	0.00155
122	0.47398	0.46501	0.79254	0.00260	0.00183
123	0.48691	0.47536	0.78143	0.00272	0.00212
124	0.49944	0.48537	0.77082	0.00285	0.00191
125	0.51243	0.49575	0.76289	0.00295	0.00167
126	0.52499	0.50579	0.75537	0.00306	0.00173
127	0.53797	0.51614	0.74762	0.00317	0.00181
128	0.55055	0.52618	0.74014	0.00328	0.00183
129	0.56351	0.53652	0.73295	0.00340	0.00183
130	0.57609	0.54655	0.72610	0.00351	0.00183
131	0.58897	0.55683	0.71956	0.00362	0.00181
132	0.60145	0.56678	0.71339	0.00373	0.00180
133	0.61415	0.57693	0.70754	0.00384	0.00178
134	0.62640	0.58671	0.70204	0.00395	0.00175
135	0.63878	0.59660	0.69688	0.00406	0.00172
136	0.65062	0.60606	0.69210	0.00416	0.00169
137	0.66245	0.61553	0.68766	0.00425	0.00164
138	0.67363	0.62448	0.68362	0.00435	0.00160
139	0.68463	0.63328	0.67992	0.00443	0.00154
140	0.69482	0.64144	0.67664	0.00451	0.00149
141	0.70460	0.64927	0.67372	0.00458	0.00142
142	0.71337	0.65630	0.67124	0.00465	0.00134
143	0.72144	0.66275	0.66318	0.00470	0.00116
144	0.72822	0.66818	0.66778	0.00474	0.00115
145	0.73395	0.67275	0.66639	0.00478	-0.00001
146	0.73804	0.67602	0.66712	0.00477	-0.00454
147	0.74066	0.67811	0.67069	0.00469	-0.00684
148	0.74134	0.67865	0.67117	0.00467	-0.00683

#### BODY COORDINATES AFTER BOUNDARY LAYER SUBTRACTION

N	XV	Y
1	0.75970	0.65171
2	0.75964	0.65167
3	0.75839	0.65070
4	0.75469	0.64793
5	0.74865	0.64345

N	XV	Y	N	XV	Y
6	0.73978	0.63696	59	0.04256	-0.01422
7	0.72825	0.62862	60	0.03730	-0.01627
8	0.71376	0.61822	61	0.03137	-0.01758
9	0.69664	0.60599	62	0.02669	-0.01749
10	0.67685	0.59186	63	0.02222	-0.01551
11	0.65492	0.57613	64	0.01885	-0.01144
12	0.63109	0.55885	65	0.01825	-0.00634
13	0.60598	0.54039	66	0.01973	-0.00105
14	0.57990	0.52087	67	0.02165	0.00355
15	0.55342	0.50065	68	0.02315	0.00655
16	0.52680	0.47987	69	0.02489	0.00969
17	0.50043	0.45882	70	0.02738	0.01386
18	0.47444	0.43757	71	0.03038	0.01861
19	0.44906	0.41633	72	0.03406	0.02410
20	0.42432	0.39512	73	0.03844	0.03036
21	0.40034	0.37401	74	0.04332	0.03707
22	0.37716	0.35301	75	0.04870	0.04427
23	0.35487	0.33213	76	0.05521	0.05177
24	0.33353	0.31140	77	0.06200	0.06025
25	0.31318	0.29085	78	0.06932	0.06936
26	0.29391	0.27055	79	0.07720	0.07901
27	0.27572	0.25050	80	0.08557	0.08912
28	0.25872	0.23079	81	0.09432	0.09958
29	0.24292	0.21143	82	0.10341	0.11031
30	0.22839	0.19265	83	0.11277	0.12125
31	0.21496	0.17453	84	0.12229	0.13224
32	0.20255	0.15739	85	0.13186	0.14319
33	0.19092	0.14125	86	0.14141	0.15401
34	0.18000	0.12628	87	0.15076	0.16449
35	0.16959	0.11237	88	0.15970	0.17442
36	0.15972	0.09958	89	0.16808	0.18364
37	0.15026	0.08777	90	0.17576	0.19201
38	0.14127	0.07697	91	0.18267	0.19947
39	0.13266	0.06702	92	0.18887	0.20612
40	0.12444	0.05785	93	0.19449	0.21208
41	0.11671	0.04951	94	0.19962	0.21748
42	0.10958	0.04216	95	0.20438	0.22245
43	0.10207	0.03454	96	0.20890	0.22713
44	0.09874	0.03125	97	0.21328	0.23163
45	0.09543	0.02810	98	0.21761	0.23605
46	0.09209	0.02498	99	0.22194	0.24045
47	0.08884	0.02200	100	0.22600	0.24454
48	0.08571	0.01917	101	0.22947	0.24800
49	0.08263	0.01640	102	0.23264	0.25113
50	0.07997	0.01334	103	0.23635	0.25479
51	0.07705	0.01086	104	0.24076	0.25912
52	0.07418	0.00847	105	0.24521	0.26316
53	0.07133	0.00614	106	0.26688	0.28386
54	0.06855	0.00391	107	0.28086	0.29693
55	0.06574	0.00172	108	0.29383	0.30872
56	0.06291	-0.00045	109	0.30787	0.32133
57	0.06027	-0.00241	110	0.32098	0.33288
58	0.04823	-0.01118	111	0.33482	0.34491

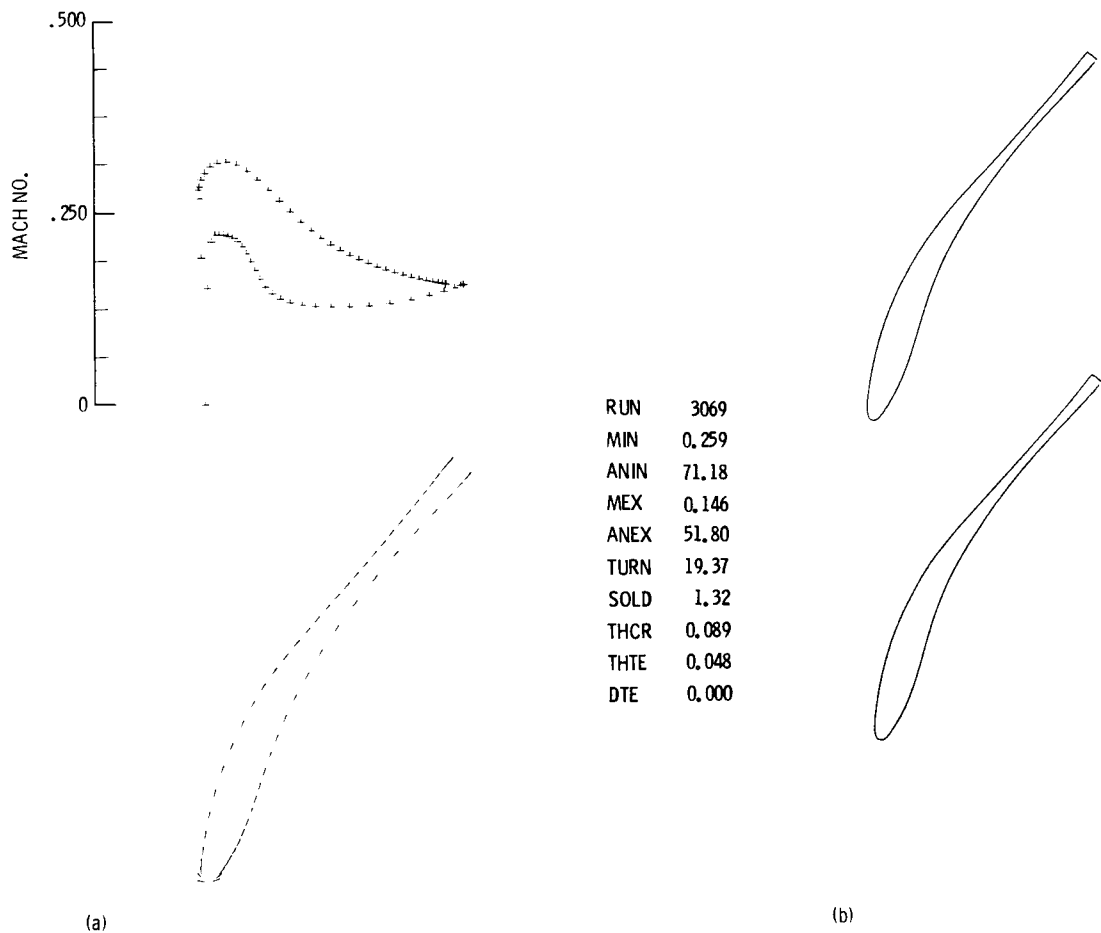
N	XV	Y
---	----	---

112	0.34781	0.35601
113	0.36141	0.36749
114	0.37423	0.37818
115	0.38760	0.38921
116	0.40028	0.39955
117	0.41349	0.41025
118	0.42608	0.42035
119	0.43918	0.43080
120	0.45173	0.44075
121	0.46476	0.45106
122	0.47731	0.46086
123	0.49038	0.47101
124	0.50305	0.48084
125	0.51618	0.49107
126	0.52886	0.50094
127	0.54196	0.51113
128	0.55468	0.52101
129	0.56777	0.53118
130	0.58048	0.54104
131	0.59349	0.55116
132	0.60609	0.56096
133	0.61892	0.57096
134	0.63128	0.58060
135	0.64377	0.59035
136	0.65571	0.59969
137	0.66764	0.60904
138	0.67891	0.61788
139	0.68998	0.62659
140	0.70025	0.63467
141	0.71008	0.64243
142	0.71890	0.64939
143	0.72699	0.65582
144	0.73379	0.66121
145	0.73949	0.66582
146	0.74345	0.66926
147	0.74598	0.67142
148	0.74660	0.67193

DXV = -0.0131; DYV = 0.0202

THICK/CHORD AT TE 0.024, DEV = 0.002

## High Stagger Subcritical Rotor



(a) Mach number distribution and inviscid airfoil.  
 (b) Relative position of airfoils in cascade plane after boundary layer is subtracted.

Figure 3.—High stagger subcritical rotor.

```

ECDATA
NRN= 3069
R= 1.80
EMACH= 0.20
THETA= 39.3750
NI= 3
NF= 64
GRID= 0.60D-01
GRIDS= 0.30D-01
IRICHD= 0
IRICHSD= 0
RN= 1000000.0
TRU= 0.70D-01
TRL= 0.60D-01
RTHO= 320.0
EEND
1

```

N	ARC	V
1	-0.375000	-0.794000
2	-0.060000	-0.658000
3	0.090000	-0.644000
4	0.271800	-0.650000
5	0.430000	-0.698000
6	0.598000	-0.867000
7	0.755000	-1.082000
8	0.790000	-1.100000
9	0.815000	-1.108000
10	0.842000	-1.102000
11	0.855000	-1.090000
12	0.862000	-1.070000

13	0.871000	-1.000000
14	0.885000	0.000000
15	0.900700	1.320000
16	0.904000	1.349000
17	0.925000	1.380000
18	0.960000	1.420000
19	1.010000	1.470000
20	1.050000	1.508000
21	1.100000	1.538000
22	1.146397	1.560000
23	1.280000	1.566000
24	1.320000	1.547000
25	1.460000	1.398000
26	1.610000	1.166500
27	1.900000	0.904000
28	2.181000	0.794000

ITER	MIN	ANIN	TURN	GAP	RESID
1	0.26	71.17	23.94	0.75	0.4089D-01
2	0.26	71.17	20.68	0.76	0.8174D-02
3	0.26	71.18	19.37	0.76	0.1633D-02

1

#### INVISCID COMPUTATION

INLET MACH NUMBER = 0.259                  INLET FLOW ANGLE = 71.18

EXIT MACH NUMBER = 0.146                  EXIT FLOW ANGLE = 51.80

TURNING = 19.372

GAP = 0.763                  CHORD = 1.007                  AXIAL CHORD = 0.548

GAP/CHORD = 0.757    SOLIDITY = 1.320    AXIAL SOLIDITY = 0.719

THICK/CHORD = 0.089,        DX = -0.0372; DY = 0.0308

THICK/CHORD AT TE = 0.048,        DEV = 0.000

N	X	Y	MACH	ANGL	CURVATURE
1	0.57180	0.82271	0.1584	50.47	0.00
2	0.57138	0.82221	0.1583	50.17	8.00
3	0.56595	0.81585	0.1568	49.02	2.39
4	0.55301	0.80128	0.1537	47.83	1.06
5	0.53131	0.77772	0.1491	46.97	0.47
6	0.50062	0.74503	0.1436	46.76	0.08
7	0.46240	0.70399	0.1379	47.43	-0.21
8	0.41973	0.65634	0.1332	48.98	-0.42
9	0.37631	0.60454	0.1302	51.12	-0.55
10	0.33510	0.55124	0.1288	53.47	-0.61
11	0.29769	0.49849	0.1285	55.87	-0.65
12	0.26477	0.44759	0.1290	58.38	-0.72
13	0.23624	0.39880	0.1305	61.03	-0.82
14	0.21207	0.35254	0.1335	63.81	-0.93
15	0.19197	0.30911	0.1383	66.51	-0.98
16	0.17542	0.26878	0.1452	68.81	-0.92
17	0.16171	0.23176	0.1540	70.46	-0.73
18	0.15006	0.19803	0.1642	71.36	-0.44
19	0.13980	0.16744	0.1754	71.43	-0.04
20	0.13010	0.13977	0.1868	70.66	0.46
21	0.12095	0.11464	0.1972	69.26	0.91
22	0.11198	0.09178	0.2065	67.37	1.34
23	0.10270	0.07093	0.2134	65.07	1.76
24	0.09337	0.05186	0.2176	62.77	1.89
25	0.08398	0.03444	0.2203	60.59	1.93
26	0.07471	0.01874	0.2218	58.19	2.29
27	0.06571	0.00497	0.2220	55.36	3.00
28	0.05734	-0.00643	0.2219	50.95	5.45
29	0.04940	-0.01484	0.2127	40.91	15.14
30	0.04163	-0.01970	0.1526	20.36	39.14
31	0.03525	-0.02021	0.0000	169.14	85.07
32	0.02863	-0.01731	0.1919	129.03	96.83
33	0.02477	-0.00807	0.2691	101.60	47.83
34	0.02352	0.00819	0.2807	89.30	13.17
35	0.02507	0.03306	0.2845	84.32	3.49
36	0.02965	0.06558	0.2935	81.08	1.72
37	0.03731	0.10696	0.3025	78.03	1.26
38	0.04863	0.15387	0.3101	74.84	1.15
39	0.06359	0.20326	0.3149	71.47	1.14
40	0.08162	0.25195	0.3161	67.84	1.22
41	0.10196	0.29763	0.3125	64.14	1.29
42	0.12373	0.33921	0.3046	60.57	1.33
43	0.14620	0.37653	0.2932	57.34	1.30
44	0.16877	0.41014	0.2798	54.57	1.19
45	0.19127	0.44048	0.2655	52.35	1.03
46	0.21345	0.46838	0.2514	50.73	0.79
47	0.23520	0.49447	0.2384	49.69	0.53
48	0.25646	0.51926	0.2270	49.13	0.30
49	0.27721	0.54313	0.2172	48.90	0.13
50	0.29748	0.56635	0.2089	48.89	0.01

51	0.31732	0.58914	0.2018	49.03	-0.08
52	0.33674	0.61154	0.1956	49.28	-0.14
53	0.35587	0.63386	0.1902	49.52	-0.15
54	0.37472	0.65605	0.1852	49.80	-0.16
55	0.39331	0.67818	0.1806	50.17	-0.22
56	0.41156	0.70021	0.1768	50.52	-0.22
57	0.42944	0.72203	0.1733	50.81	-0.18
58	0.44686	0.74350	0.1701	51.08	-0.17
59	0.46368	0.76442	0.1673	51.31	-0.15
60	0.47970	0.78450	0.1650	51.48	-0.12
61	0.49463	0.80329	0.1629	51.59	-0.08
62	0.50808	0.82027	0.1613	51.62	-0.02
63	0.51955	0.83473	0.1601	51.55	0.07
64	0.52834	0.84577	0.1592	51.35	0.24
65	0.53357	0.85227	0.1587	50.95	0.84
66	0.53456	0.85348	0.1584	50.47	5.37

1

BOUNDARY LAYER CORRECTION  
PRESSURE SIDE

N	X	Y	EM	TH	SEP
31	0.03525	-0.02021	0.00002		
30	0.04163	-0.01970	0.15258		
29	0.04940	-0.01484	0.21267		
28	0.05734	-0.00643	0.22189		
27	0.06571	0.00497	0.22198	0.00029	0.00009
26	0.07471	0.01874	0.22184	0.00034	0.00008
25	0.08398	0.03444	0.22030	0.00040	0.00022
24	0.09337	0.05186	0.21765	0.00047	0.00039
23	0.10270	0.07093	0.21344	0.00056	0.00073
22	0.11188	0.09178	0.20649	0.00067	0.00124
21	0.12095	0.11464	0.19722	0.00083	0.00181
20	0.13010	0.13977	0.18677	0.00104	0.00244
19	0.13980	0.16744	0.17543	0.00132	0.00310
18	0.15006	0.19803	0.16420	0.00169	0.00362
17	0.16171	0.23176	0.15399	0.00214	0.00388
16	0.17542	0.26878	0.14523	0.00266	0.00377
15	0.19197	0.30911	0.13830	0.00321	0.00318
14	0.21207	0.35254	0.13347	0.00370	0.00225
13	0.23624	0.39880	0.13052	0.00406	0.00133
12	0.26477	0.44759	0.12899	0.00429	0.00060
11	0.29769	0.49849	0.12847	0.00442	0.00006
10	0.33510	0.55124	0.12882	0.00446	-0.00044
9	0.37631	0.60454	0.13023	0.00440	-0.00105
8	0.41973	0.65634	0.13324	0.00417	-0.00173
7	0.46240	0.70399	0.13790	0.00382	-0.00226
6	0.50062	0.74503	0.14355	0.00344	-0.00256
5	0.53131	0.77772	0.14913	0.00312	-0.00270
4	0.55301	0.80128	0.15374	0.00290	-0.00277
3	0.56595	0.81585	0.15681	0.00277	-0.00292
2	0.57138	0.82221	0.15826	0.00271	-0.00297
1	0.57180	0.82271	0.15844	0.00270	-0.00297

SUCTION SIDE

N	X	Y	EM	TH	SEP
32	0.02863	-0.01731	0.19189		
33	0.02477	-0.00807	0.26907		
34	0.02352	0.00819	0.28065		
35	0.02507	0.03306	0.28452		
36	0.02965	0.06558	0.29352		
37	0.03731	0.10696	0.30249		
38	0.04863	0.15387	0.31013		
39	0.06359	0.20326	0.31485		
40	0.08162	0.25195	0.31606	0.00021	0.00009
41	0.10196	0.29763	0.31246	0.00037	0.00018
42	0.12373	0.33921	0.30460	0.00051	0.00043
43	0.14620	0.37653	0.29322	0.00067	0.00079
44	0.16877	0.41014	0.27984	0.00086	0.00124
45	0.19127	0.44048	0.26550	0.00109	0.00177
46	0.21345	0.46838	0.25141	0.00135	0.00230
47	0.23520	0.49447	0.23837	0.00165	0.00275
48	0.25646	0.51926	0.22699	0.00198	0.00307
49	0.27721	0.54313	0.21725	0.00233	0.00329
50	0.29748	0.56635	0.20895	0.00270	0.00346
51	0.31732	0.58914	0.20177	0.00308	0.00357
52	0.33674	0.61154	0.19561	0.00347	0.00363
53	0.35587	0.63386	0.19021	0.00387	0.00380
54	0.37472	0.65605	0.18515	0.00429	0.00399
55	0.39331	0.67818	0.18060	0.00473	0.00395
56	0.41156	0.70021	0.17675	0.00515	0.00389
57	0.42944	0.72203	0.17326	0.00558	0.00394
58	0.44686	0.74350	0.17011	0.00600	0.00393
59	0.46368	0.76442	0.16734	0.00642	0.00384
60	0.47970	0.78450	0.16495	0.00680	0.00370
61	0.49463	0.80329	0.16294	0.00715	0.00352
62	0.50808	0.82027	0.16132	0.00745	0.00332
63	0.51955	0.83473	0.16007	0.00770	0.00311
64	0.52834	0.84577	0.15921	0.00787	0.00294
65	0.53357	0.85227	0.15872	0.00797	0.00290
66	0.53456	0.85348	0.15844	0.00799	0.00290

BODY COORDINATES AFTER BOUNDARY LAYER SUBTRACTION

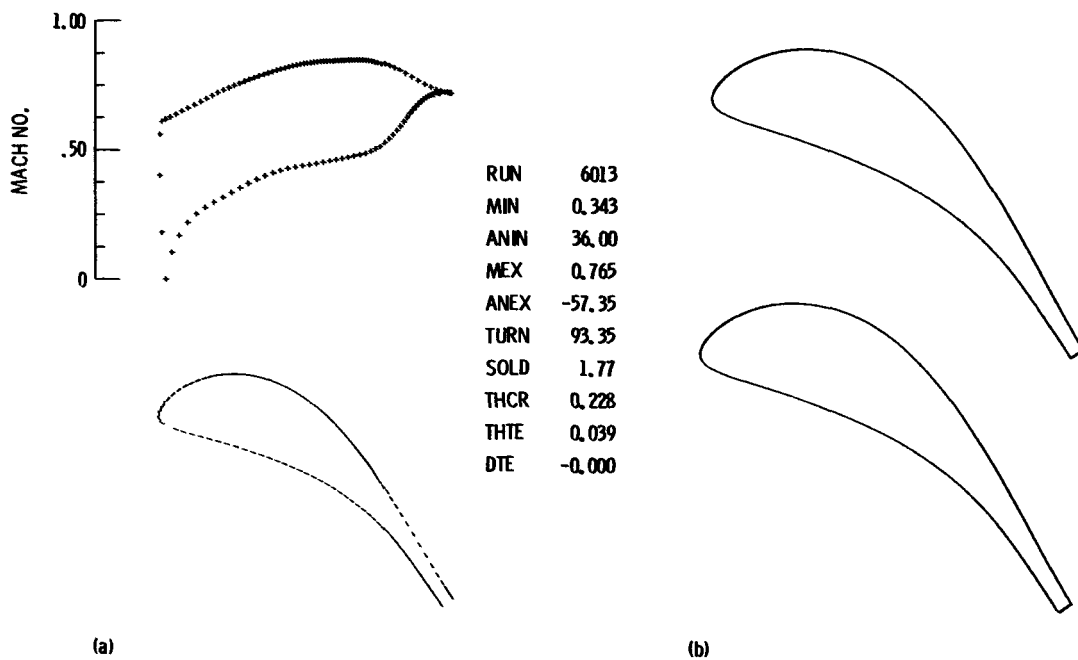
N	XV	Y	N	XV	Y
1	0.56931	0.82476	6	0.49776	0.74772
2	0.56890	0.82427	7	0.45911	0.70702
3	0.56350	0.81798	8	0.41583	0.65974
4	0.55053	0.80353	9	0.37172	0.60824
5	0.52870	0.78015	10	0.32986	0.55512

N	XV	Y	N	XV	Y
11	0.29188	0.50243	41	0.10270	0.29728
12	0.25839	0.45152	42	0.12465	0.33869
13	0.22932	0.40263	43	0.14732	0.37581
14	0.20489	0.35607	44	0.17014	0.40917
15	0.18510	0.31209	45	0.19297	0.43917
16	0.16943	0.27110	46	0.21556	0.46665
17	0.15687	0.23348	47	0.23779	0.49227
18	0.14633	0.19929	48	0.25958	0.51656
19	0.13698	0.16839	49	0.28091	0.53989
20	0.12799	0.14051	50	0.30181	0.56257
21	0.11936	0.11525	51	0.32232	0.58480
22	0.11066	0.09229	52	0.34244	0.60663
23	0.10174	0.07138	53	0.36232	0.62836
24	0.09259	0.05226	54	0.38197	0.64993
25	0.08333	0.03480	55	0.40138	0.67145
26	0.07417	0.01907	56	0.42046	0.69288
27	0.06533	0.00524	57	0.43915	0.71411
28	0.05734	-0.00643	58	0.45738	0.73501
29	0.04940	-0.01484	59	0.47495	0.75539
30	0.04163	-0.01970	60	0.49163	0.77500
31	0.03525	-0.02021	61	0.50710	0.79340
32	0.02863	-0.01731	62	0.52095	0.81008
33	0.02477	-0.00807	63	0.53264	0.82433
34	0.02352	0.00819	64	0.54150	0.83524
35	0.02507	0.03306	65	0.54663	0.84168
36	0.02965	0.06558	66	0.54752	0.84279
37	0.03731	0.10696			
38	0.04863	0.15387			
39	0.06359	0.20326			
40	0.08194	0.25182			

DXV = -0.0218; DYV = 0.0180

THICK/CHORD AT TE 0.028, DEV = 0.000

## Subcritical Turbine Blade



(a) Mach number distribution and inviscid airfoil.  
 (b) Relative position of airfoils in cascade plane after boundary layer is subtracted.

Figure 4.—Subcritical turbine blade.

	N	ARC	V
EDATA			
NRN= 6013			
R= 1.40	1	-1.272000	-1.940000
EMACH= 0.360	2	-1.144000	-1.850000
THETA= 9.0	3	-1.018000	-1.620000
NI= 3	4	-0.927300	-1.460000
NF= 128	5	-0.814100	-1.358000
GRID= 0.60D-01	6	-0.663500	-1.286000
GRIDS= 0.40D-01	7	-0.571900	-1.242000
IRICHd= 1	8	-0.440300	-1.179000
IRICHs= 0	9	-0.310600	-1.042000
RN= 1000000.0	10	-0.229400	-0.930000
TRU= 0.230	11	-0.120400	-0.771000
TRL= -0.90D-01	12	-0.027000	-0.488000
RTH0= 320.0	13	0.006000	-0.284400
EEND	14	0.029000	0.000000
1	15	0.080000	1.500000
	16	0.086890	1.535000
	17	0.098000	1.565000
	18	0.126000	1.620000
	19	0.151600	1.660000
	20	0.175000	1.690000

21	0.185000	1.706000
22	0.231000	1.766000
23	0.305800	1.861000
24	0.437200	2.012000
25	0.567800	2.125000
26	0.711500	2.208000
27	0.878700	2.240000
28	1.072000	2.242000
29	1.318000	2.131000
30	1.536000	1.986000
31	1.681000	1.940000

ITER	MIN	ANIN	TURN	GAP	RESID
1	0.33	36.17	95.15	0.60	0.1789D 00
2	0.34	36.06	93.85	0.60	0.3504D-01
3	0.34	36.00	93.35	0.60	0.6561D-02

1

#### INVISCID COMPUTATION

INLET MACH NUMBER = 0.343      INLET FLOW ANGLE = 36.00

EXIT MACH NUMBER = 0.765      EXIT FLOW ANGLE = -57.35

TURNING = 93.353

GAP = 0.603      CHORD = 1.066      AXIAL CHORD = 0.903

GAP/CHORD = 0.566      SOLIDITY = 1.767      AXIAL SOLIDITY = 1.497

THICK/CHORD = 0.228,      DX = 0.0342; DY = 0.0232

THICK/CHORD AT TE = 0.039,      DEV = -0.000

N	X	Y	MACH	ANGL	CURVATURE
1	0.68899	-0.74935	0.7248	-56.11	0.00
2	0.68899	-0.74935	0.7248	-56.11	0.00
3	0.68811	-0.74804	0.7247	-55.82	-3.21
4	0.68581	-0.74467	0.7246	-55.56	-1.13
5	0.68235	-0.73966	0.7242	-55.32	-0.68
6	0.67797	-0.73335	0.7234	-55.10	-0.48
7	0.67283	-0.72601	0.7220	-54.92	-0.37
8	0.66708	-0.71784	0.7197	-54.75	-0.29
9	0.66080	-0.70899	0.7165	-54.60	-0.24
10	0.65409	-0.69957	0.7122	-54.47	-0.20
11	0.64700	-0.68966	0.7067	-54.34	-0.18
12	0.63955	-0.67931	0.6998	-54.22	-0.17
13	0.63178	-0.66855	0.6915	-54.09	-0.17
14	0.62370	-0.65741	0.6817	-53.95	-0.18
15	0.61528	-0.64589	0.6703	-53.76	-0.22
16	0.60653	-0.63400	0.6574	-53.53	-0.28
17	0.59741	-0.62173	0.6433	-53.22	-0.35
18	0.58788	-0.60908	0.6281	-52.82	-0.44
19	0.57791	-0.59605	0.6120	-52.29	-0.56
20	0.56744	-0.58266	0.5953	-51.63	-0.68
21	0.55641	-0.56892	0.5785	-50.79	-0.83
22	0.54474	-0.55488	0.5618	-49.75	-0.99
23	0.53238	-0.54059	0.5461	-48.48	-1.17
24	0.51926	-0.52614	0.5319	-47.00	-1.33
25	0.50536	-0.51167	0.5208	-45.30	-1.47
26	0.49073	-0.49730	0.5126	-43.74	-1.33
27	0.47542	-0.48303	0.5026	-42.19	-1.29
28	0.45934	-0.46891	0.4943	-40.35	-1.50
29	0.44256	-0.45510	0.4888	-38.61	-1.40
30	0.42514	-0.44160	0.4834	-36.95	-1.32
31	0.40711	-0.42844	0.4784	-35.31	-1.28
32	0.38850	-0.41564	0.4735	-33.73	-1.22
33	0.36931	-0.40320	0.4685	-32.18	-1.18
34	0.34956	-0.39114	0.4633	-30.66	-1.15
35	0.32924	-0.37946	0.4578	-29.13	-1.14
36	0.30835	-0.36818	0.4525	-27.60	-1.13
37	0.28692	-0.35734	0.4474	-26.10	-1.09
38	0.26500	-0.34694	0.4426	-24.69	-1.01
39	0.24262	-0.33695	0.4376	-23.44	-0.89
40	0.21982	-0.32733	0.4316	-22.36	-0.76
41	0.19658	-0.31799	0.4240	-21.45	-0.63
42	0.17284	-0.30885	0.4143	-20.66	-0.55
43	0.14854	-0.29987	0.4023	-19.91	-0.50
44	0.12357	-0.29102	0.3882	-19.15	-0.50
45	0.09789	-0.28229	0.3722	-18.35	-0.52
46	0.07140	-0.27374	0.3548	-17.43	-0.57
47	0.04416	-0.26545	0.3365	-16.40	-0.63
48	0.01625	-0.25752	0.3181	-15.36	-0.63
49	-0.01200	-0.24999	0.2989	-14.56	-0.48
50	-0.04025	-0.24277	0.2780	-14.22	-0.20

51	-0.06793	-0.23565	0.2527	-14.80	0.35
52	-0.09462	-0.22821	0.2185	-16.62	1.15
53	-0.11980	-0.22005	0.1693	-19.31	1.78
54	-0.14312	-0.21130	0.1038	-22.19	2.01
55	-0.16123	-0.20287	0.0000	-211.51	322.66
56	-0.17406	-0.19174	0.1826	127.19	-348.22
57	-0.17983	-0.17877	0.4032	100.65	32.62
58	-0.17936	-0.16431	0.5635	76.78	28.80
59	-0.17301	-0.14898	0.6126	60.11	17.53
60	-0.16168	-0.13297	0.6186	50.33	8.70
61	-0.14674	-0.11708	0.6276	43.54	5.43
62	-0.12944	-0.10221	0.6383	37.98	4.25
63	-0.11078	-0.08891	0.6505	33.07	3.74
64	-0.09251	-0.07865	0.6627	28.53	3.78
65	-0.07308	-0.06899	0.6751	24.31	3.40
66	-0.05381	-0.06109	0.6878	20.29	3.37
67	-0.03491	-0.05481	0.7003	16.44	3.37
68	-0.01644	-0.05000	0.7122	12.77	3.36
69	0.00155	-0.04650	0.7233	9.26	3.34
70	0.01907	-0.04417	0.7337	5.92	3.29
71	0.03612	-0.04288	0.7434	2.76	3.23
72	0.05271	-0.04251	0.7525	-0.25	3.16
73	0.06887	-0.04299	0.7610	-3.10	3.08
74	0.08462	-0.04422	0.7689	-5.81	2.99
75	0.09997	-0.04613	0.7763	-8.39	2.91
76	0.11494	-0.04867	0.7832	-10.84	2.82
77	0.12954	-0.05178	0.7897	-13.18	2.74
78	0.14379	-0.05541	0.7959	-15.42	2.66
79	0.15770	-0.05953	0.8017	-17.58	2.59
80	0.17128	-0.06410	0.8072	-19.64	2.52
81	0.18453	-0.06910	0.8125	-21.64	2.46
82	0.19746	-0.07448	0.8174	-23.57	2.40
83	0.21008	-0.08023	0.8220	-25.43	2.35
84	0.22239	-0.08633	0.8263	-27.24	2.29
85	0.23441	-0.09275	0.8302	-28.98	2.24
86	0.24613	-0.09947	0.8338	-30.67	2.18
87	0.25757	-0.10648	0.8370	-32.31	2.13
88	0.26873	-0.11375	0.8399	-33.88	2.07
89	0.27962	-0.12128	0.8421	-35.41	2.01
90	0.29025	-0.12905	0.8437	-36.85	1.91
91	0.30064	-0.13703	0.8459	-38.23	1.84
92	0.31078	-0.14521	0.8478	-39.57	1.80
93	0.32067	-0.15357	0.8489	-40.84	1.71
94	0.33035	-0.16212	0.8500	-42.05	1.62
95	0.33981	-0.17083	0.8508	-43.18	1.54
96	0.34908	-0.17969	0.8516	-44.26	1.46
97	0.35815	-0.18869	0.8522	-45.27	1.38
98	0.36705	-0.19782	0.8529	-46.22	1.30
99	0.37579	-0.20709	0.8535	-47.11	1.23
100	0.38438	-0.21648	0.8541	-47.96	1.15
101	0.39285	-0.22601	0.8546	-48.75	1.09
102	0.40122	-0.23567	0.8551	-49.50	1.02
103	0.40951	-0.24550	0.8555	-50.21	0.96
104	0.41775	-0.25551	0.8558	-50.88	0.90
105	0.42597	-0.26574	0.8559	-51.52	0.85

106	0.43422	-0.27624	0.8559	-52.13	0.80
107	0.44255	-0.28706	0.8556	-52.72	0.75
108	0.45101	-0.29829	0.8550	-53.28	0.70
109	0.45966	-0.31001	0.8541	-53.83	0.66
110	0.46860	-0.32236	0.8527	-54.37	0.61
111	0.47792	-0.33549	0.8508	-54.89	0.57
112	0.48773	-0.34958	0.8483	-55.41	0.52
113	0.49817	-0.36487	0.8450	-55.91	0.48
114	0.50941	-0.38163	0.8409	-56.41	0.43
115	0.52162	-0.40020	0.8356	-56.90	0.39
116	0.53500	-0.42091	0.8291	-57.38	0.34
117	0.54973	-0.44413	0.8209	-57.84	0.29
118	0.56594	-0.47014	0.8109	-58.27	0.24
119	0.58366	-0.49901	0.7990	-58.63	0.19
120	0.60273	-0.53045	0.7855	-58.88	0.12
121	0.62269	-0.56361	0.7712	-58.98	0.05
122	0.64279	-0.59701	0.7576	-58.91	-0.03
123	0.66202	-0.62877	0.7462	-58.67	-0.11
124	0.67934	-0.65704	0.7377	-58.32	-0.19
125	0.69396	-0.68056	0.7320	-57.92	-0.25
126	0.70548	-0.69880	0.7285	-57.51	-0.33
127	0.71387	-0.71188	0.7265	-57.12	-0.44
128	0.71938	-0.72034	0.7255	-56.76	-0.63
129	0.72236	-0.72487	0.7249	-56.42	-1.09
130	0.72323	-0.72617	0.7248	-56.11	-3.51

1

#### BOUNDARY LAYER CORRECTION

#### PRESSURE SIDE

N	X	Y	EM	TH	SEP
55	-0.16123	-0.20287	0.00003		
54	-0.14312	-0.21130	0.10382		
53	-0.11980	-0.22005	0.16933		
52	-0.09462	-0.22821	0.21852		
51	-0.06793	-0.23565	0.25272	0.00063	0.00009
50	-0.04025	-0.24277	0.27800	0.00051	-0.00150
49	-0.01200	-0.24999	0.29893	0.00055	-0.00127
48	0.01625	-0.25752	0.31807	0.00057	-0.00118
47	0.04416	-0.26545	0.33648	0.00061	-0.00116
46	0.07140	-0.27374	0.35475	0.00064	-0.00114
45	0.09789	-0.28229	0.37218	0.00067	-0.00108
44	0.12357	-0.29102	0.38817	0.00070	-0.00100
43	0.14854	-0.29987	0.40225	0.00073	-0.00090
42	0.17284	-0.30885	0.41428	0.00077	-0.00079
41	0.19658	-0.31799	0.42403	0.00082	-0.00066
40	0.21982	-0.32733	0.43163	0.00087	-0.00054

39	0.24262	-0.33695	0.43758	0.00093	-0.00047
38	0.26500	-0.34694	0.44261	0.00098	-0.00044
37	0.28692	-0.35734	0.44739	0.00103	-0.00046
36	0.30835	-0.36818	0.45245	0.00108	-0.00051
35	0.32924	-0.37946	0.45784	0.00112	-0.00055
34	0.34956	-0.39114	0.46328	0.00116	-0.00056
33	0.36931	-0.40320	0.46850	0.00119	-0.00055
32	0.38850	-0.41564	0.47346	0.00123	-0.00054
31	0.40711	-0.42844	0.47837	0.00126	-0.00056
30	0.42514	-0.44160	0.48336	0.00129	-0.00060
29	0.44256	-0.45510	0.48879	0.00131	-0.00065
28	0.45934	-0.46891	0.49432	0.00133	-0.00082
27	0.47542	-0.48303	0.50258	0.00133	-0.00108
26	0.49073	-0.49730	0.51256	0.00131	-0.00107
25	0.50536	-0.51167	0.52084	0.00131	-0.00113
24	0.51926	-0.52614	0.53192	0.00129	-0.00144
23	0.53238	-0.54059	0.54614	0.00125	-0.00165
22	0.54474	-0.55488	0.56182	0.00121	-0.00173
21	0.55641	-0.56892	0.57848	0.00116	-0.00173
20	0.56744	-0.58266	0.59533	0.00113	-0.00169
19	0.57791	-0.59605	0.61202	0.00110	-0.00162
18	0.58788	-0.60908	0.62809	0.00107	-0.00152
17	0.59741	-0.62173	0.64333	0.00105	-0.00142
16	0.60653	-0.63400	0.65744	0.00104	-0.00131
15	0.61528	-0.64589	0.67028	0.00104	-0.00119
14	0.62370	-0.65741	0.68166	0.00104	-0.00106
13	0.63178	-0.66855	0.69152	0.00105	-0.00093
12	0.63955	-0.67931	0.69982	0.00106	-0.00081
11	0.64700	-0.68966	0.70669	0.00107	-0.00069
10	0.65409	-0.69957	0.71222	0.00109	-0.00058
9	0.66080	-0.70899	0.71652	0.00111	-0.00047
8	0.66708	-0.71784	0.71972	0.00113	-0.00037
7	0.67283	-0.72601	0.72196	0.00115	-0.00028
6	0.67797	-0.73335	0.72339	0.00118	-0.00019
5	0.68235	-0.73966	0.72420	0.00120	-0.00012
4	0.68581	-0.74467	0.72457	0.00121	-0.00007
3	0.68811	-0.74804	0.72469	0.00123	-0.00006
2	0.68899	-0.74935	0.72476	0.00123	-0.00006
1	0.68899	-0.74935	0.72476	0.00123	-0.00006

### SUCTION SIDE

N	X	Y	EM	TH	SEP
56	-0.17406	-0.19174	0.18260		
57	-0.17983	-0.17877	0.40325		
58	-0.17936	-0.16431	0.56347		
59	-0.17301	-0.14898	0.61257		
60	-0.16168	-0.13297	0.61864		
61	-0.14674	-0.11708	0.62760		
62	-0.12944	-0.10221	0.63826		

63	-0.11078	-0.08891	0.65053		
64	-0.09251	-0.07865	0.66270		
65	-0.07308	-0.06899	0.67505		
66	-0.05381	-0.06109	0.68781		
67	-0.03491	-0.05481	0.70029		
68	-0.01644	-0.05000	0.71216		
69	0.00155	-0.04650	0.72329		
70	0.01907	-0.04417	0.73372		
71	0.03612	-0.04288	0.74345		
72	0.05271	-0.04251	0.75254		
73	0.06887	-0.04299	0.76100		
74	0.08462	-0.04422	0.76891		
75	0.09997	-0.04613	0.77629		
76	0.11494	-0.04867	0.78323		
77	0.12954	-0.05178	0.78974		
78	0.14379	-0.05541	0.79590		
79	0.15770	-0.05953	0.80171		
80	0.17128	-0.06410	0.80724		
81	0.18453	-0.06910	0.81246		
82	0.19746	-0.07448	0.81738		
83	0.21008	-0.08023	0.82198		
84	0.22239	-0.08633	0.82627		
85	0.23441	-0.09275	0.83019	0.00025	0.00007
86	0.24613	-0.09947	0.83380	0.00028	-0.00008
87	0.25757	-0.10648	0.83700	0.00032	-0.00008
88	0.26873	-0.11375	0.83986	0.00035	-0.00007
89	0.27962	-0.12128	0.84206	0.00038	-0.00006
90	0.29025	-0.12905	0.84370	0.00041	-0.00007
91	0.30064	-0.13703	0.84594	0.00044	-0.00007
92	0.31078	-0.14521	0.84782	0.00047	-0.00006
93	0.32067	-0.15357	0.84892	0.00050	-0.00004
94	0.33035	-0.16212	0.84996	0.00052	-0.00004
95	0.33981	-0.17083	0.85080	0.00055	-0.00004
96	0.34908	-0.17969	0.85156	0.00058	-0.00003
97	0.35815	-0.18869	0.85222	0.00061	-0.00003
98	0.36705	-0.19782	0.85286	0.00063	-0.00003
99	0.37579	-0.20709	0.85348	0.00066	-0.00003
100	0.38438	-0.21648	0.85408	0.00068	-0.00003
101	0.39285	-0.22601	0.85464	0.00071	-0.00003
102	0.40122	-0.23567	0.85513	0.00073	-0.00003
103	0.40951	-0.24550	0.85552	0.00076	-0.00002
104	0.41775	-0.25551	0.85580	0.00079	-0.00001
105	0.42597	-0.26574	0.85592	0.00081	-0.00000
106	0.43422	-0.27624	0.85586	0.00084	0.00001
107	0.44255	-0.28706	0.85556	0.00087	0.00003
108	0.45101	-0.29829	0.85499	0.00089	0.00005
109	0.45966	-0.31001	0.85406	0.00093	0.00007
110	0.46860	-0.32236	0.85270	0.00096	0.00010
111	0.47792	-0.33549	0.85080	0.00099	0.00014
112	0.48773	-0.34958	0.84829	0.00103	0.00018
113	0.49817	-0.36487	0.84502	0.00108	0.00022
114	0.50941	-0.38163	0.84087	0.00113	0.00027
115	0.52162	-0.40020	0.83563	0.00119	0.00032
116	0.53500	-0.42091	0.82907	0.00125	0.00039

117	0.54973	-0.44413	0.82091	0.00133	0.00046
118	0.56594	-0.47014	0.81093	0.00143	0.00055
119	0.58366	-0.49901	0.79901	0.00154	0.00064
120	0.60273	-0.53045	0.78546	0.00167	0.00073
121	0.62269	-0.56361	0.77121	0.00181	0.00078
122	0.64279	-0.59701	0.75765	0.00196	0.00079
123	0.66202	-0.62877	0.74618	0.00210	0.00073
124	0.67934	-0.65704	0.73765	0.00221	0.00063
125	0.69396	-0.68056	0.73196	0.00230	0.00052
126	0.70548	-0.69880	0.72848	0.00236	0.00042
127	0.71387	-0.71188	0.72650	0.00240	0.00034
128	0.71938	-0.72034	0.72545	0.00242	0.00029
129	0.72236	-0.72487	0.72495	0.00243	0.00028
130	0.72323	-0.72617	0.72476	0.00244	0.00028

#### BODY COORDINATES AFTER BOUNDARY LAYER SUBTRACTION

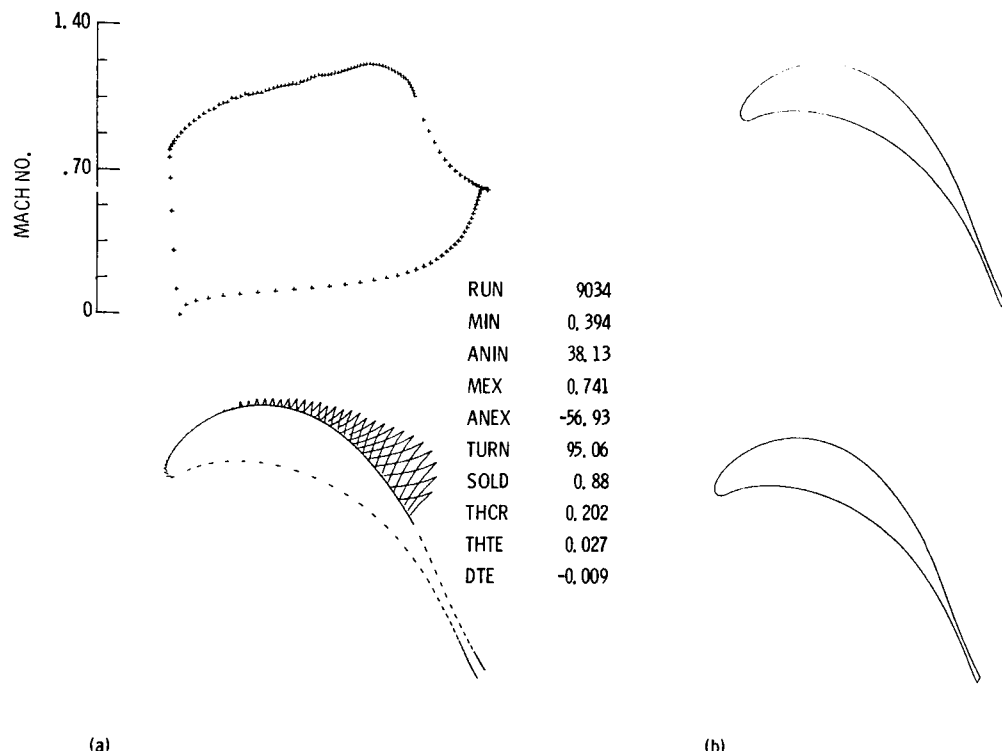
N	XV	Y	N	XV	Y
1	0.69040	-0.74840	31	0.40810	-0.42705
2	0.69040	-0.74840	32	0.38942	-0.41426
3	0.68952	-0.74709	33	0.37017	-0.40183
4	0.68720	-0.74371	34	0.35036	-0.38979
5	0.68373	-0.73871	35	0.32998	-0.37813
6	0.67932	-0.73241	36	0.30903	-0.36688
7	0.67416	-0.72508	37	0.28755	-0.35607
8	0.66837	-0.71693	38	0.26556	-0.34571
9	0.66207	-0.70809	39	0.24313	-0.33578
10	0.65533	-0.69869	40	0.22027	-0.32621
11	0.64820	-0.68879	41	0.19699	-0.31693
12	0.64074	-0.67845	42	0.17321	-0.30786
13	0.63294	-0.66771	43	0.14888	-0.29893
14	0.62484	-0.65658	44	0.12389	-0.29012
15	0.61641	-0.64506	45	0.09818	-0.28143
16	0.60765	-0.63317	46	0.07166	-0.27291
17	0.59853	-0.62089	47	0.04439	-0.26465
18	0.58901	-0.60822	48	0.01646	-0.25674
19	0.57904	-0.59518	49	-0.01181	-0.24925
20	0.56859	-0.58175	50	-0.04006	-0.24200
21	0.55757	-0.56797	51	-0.06767	-0.23468
22	0.54592	-0.55388	52	-0.09462	-0.22821
23	0.53358	-0.53952	53	-0.11980	-0.22005
24	0.52048	-0.52501	54	-0.14312	-0.21130
25	0.50658	-0.51046	55	-0.16123	-0.20287
26	0.49194	-0.49604	56	-0.17406	-0.19174
27	0.47660	-0.48173	57	-0.17983	-0.17877
28	0.46049	-0.46756	58	-0.17936	-0.16431
29	0.44366	-0.45371	59	-0.17301	-0.14898
30	0.42619	-0.44021	60	-0.16168	-0.13297
			61	-0.14674	-0.11708
			62	-0.12944	-0.10221
			63	-0.11078	-0.08891

N	XV	Y	N	XV	Y
64	-0.09251	-0.07865	100	0.38344	-0.21733
65	-0.07308	-0.06899	101	0.39186	-0.22687
66	-0.05381	-0.06109	102	0.40019	-0.23655
67	-0.03491	-0.05481	103	0.40843	-0.24640
68	-0.01644	-0.05000	104	0.41663	-0.25643
69	0.00155	-0.04650	105	0.42480	-0.26667
70	0.01907	-0.04417	106	0.43301	-0.27719
71	0.03612	-0.04288	107	0.44129	-0.28803
72	0.05271	-0.04251	108	0.44969	-0.29927
73	0.06887	-0.04299	109	0.45829	-0.31102
74	0.08462	-0.04422	110	0.46717	-0.32339
75	0.09997	-0.04613	111	0.47642	-0.33654
76	0.11494	-0.04867	112	0.48616	-0.35066
77	0.12954	-0.05178	113	0.49652	-0.36599
78	0.14379	-0.05541	114	0.50766	-0.38280
79	0.15770	-0.05953	115	0.51976	-0.40141
80	0.17128	-0.06410	116	0.53301	-0.42218
81	0.18453	-0.06910	117	0.54759	-0.44548
82	0.19746	-0.07448	118	0.56362	-0.47157
83	0.21008	-0.08023	119	0.58114	-0.50054
84	0.22239	-0.08633	120	0.59999	-0.53211
85	0.23418	-0.09316	121	0.61973	-0.56540
86	0.24583	-0.09999	122	0.63962	-0.59892
87	0.25722	-0.10703	123	0.65869	-0.63079
88	0.26834	-0.11434	124	0.67591	-0.65916
89	0.27918	-0.12190	125	0.69048	-0.68274
90	0.28977	-0.12969	126	0.70198	-0.70103
91	0.30011	-0.13770	127	0.71036	-0.71415
92	0.31020	-0.14591	128	0.71588	-0.72263
93	0.32005	-0.15430	129	0.71888	-0.72718
94	0.32968	-0.16286	130	0.71976	-0.72850
95	0.33909	-0.17159			
96	0.34831	-0.18047			
97	0.35734	-0.18949			
98	0.36619	-0.19864			
99	0.37489	-0.20792			

DXV = 0.0294; DYV = 0.0199

THICK/CHORD AT TE 0.033, DEV = -0.000

## Supercritical Turbine Blade



(a) Mach number distribution and inviscid airfoil.  
 (b) Relative position of airfoils in cascade plane after boundary layer is subtracted.

Figure 5.—Supercritical turbine blade.

	N	ARC	V
E DATA	1	-1.771000	-1.580000
NRN= 9034	2	-1.675000	-1.220000
R= 2.050	3	-1.590000	-1.030000
EMACH= 0.3750	4	-1.350000	-0.720000
THETA= 23.0	5	-1.118000	-0.540000
NI= 3	6	-0.864100	-0.420000
NF= 128	7	-0.611900	-0.345000
GRID= 0.60D-01	8	-0.449300	-0.305000
GRIDS= 0.40D-01	9	-0.310600	-0.272000
IRICHD= 1	10	-0.160400	-0.230000
IRICHSD= 1	11	-0.042400	-0.171000
RN= 1000000.0	12	0.021000	-0.008000
TRU= 0.360	13	0.030000	0.110000
TRL= 0.40	14	0.033000	0.200000
RTHO= 320.0	15	0.080000	1.800000
E END	16	0.086890	1.895000
1	17	0.098000	1.958000
	18	0.143600	2.070000
	19	0.218000	2.216000

20	0.295800	2.341000
21	0.437200	2.512000
22	0.567800	2.645000
23	0.711500	2.758000
24	0.878700	2.865000
25	1.072000	2.943000
26	1.318000	2.924000
27	1.370000	2.845000
28	1.656000	2.150000
29	1.960000	1.740000
30	2.221000	1.580000

ITER	MIN	ANIN	TURN	GAP	RESID
1	0.38	38.82	97.91	1.18	0.2154D 00
2	0.39	38.36	95.95	1.19	0.3796D-01
3	0.39	38.13	95.06	1.19	0.6594D-02

1

INVISCID	COMPUTATION
INLET MACH NUMBER = 0.394	INLET FLOW ANGLE = 38.13
EXIT MACH NUMBER = 0.741	EXIT FLOW ANGLE = 56.93
TURNING = 95.058	
GAP = 1.191	CHORD = 1.052
AXIAL CHORD = 0.883	
GAP/CHORD = 1.132 SOLIDITY = 0.883 AXIAL SOLIDITY = 0.742	
THICK/CHORD = 0.202, DX = 0.0195; DY = 0.0230	
THICK/CHORD AT TE = 0.027, DEV = -0.009	

N	X	Y	MACH	ANGL	CURVATURE
1	0.69651	-0.75853	0.6051	-59.18	0.00
2	0.69651	-0.75853	0.6051	-59.18	0.00
3	0.69618	-0.75798	0.6030	-59.74	15.37
4	0.69475	-0.75548	0.5963	-60.52	4.72
5	0.69300	-0.75233	0.5855	-61.37	4.13
6	0.69032	-0.74733	0.5710	-62.25	2.70
7	0.68743	-0.74171	0.5535	-63.10	2.33
8	0.68369	-0.73423	0.5334	-63.87	1.61
9	0.67978	-0.72612	0.5114	-64.51	1.25
10	0.67503	-0.71606	0.4881	-64.99	0.75
11	0.67007	-0.70534	0.4644	-65.25	0.39
12	0.66420	-0.69259	0.4411	-65.29	0.06
13	0.65801	-0.67915	0.4186	-65.16	-0.16
14	0.65078	-0.66364	0.3967	-64.91	-0.26
15	0.64312	-0.64742	0.3745	-64.48	-0.41
16	0.63417	-0.62901	0.3533	-63.66	-0.70
17	0.62454	-0.60997	0.3347	-62.63	-0.85
18	0.61338	-0.58888	0.3179	-61.68	-0.69
19	0.60155	-0.56724	0.3007	-60.99	-0.49
20	0.58804	-0.54330	0.2813	-60.08	-0.57
21	0.57339	-0.51855	0.2626	-58.59	-0.91
22	0.55634	-0.49158	0.2455	-56.87	-0.94
23	0.53772	-0.46404	0.2289	-54.92	-1.02
24	0.51606	-0.43447	0.2131	-52.64	-1.09
25	0.49224	-0.40469	0.1981	-49.97	-1.22
26	0.46455	-0.37347	0.1843	-46.90	-1.28
27	0.43417	-0.34287	0.1717	-43.45	-1.40
28	0.39933	-0.31200	0.1603	-39.66	-1.42
29	0.36172	-0.28299	0.1500	-35.58	-1.50
30	0.31967	-0.25525	0.1407	-31.25	-1.50
31	0.27545	-0.23074	0.1321	-26.71	-1.57
32	0.22754	-0.20907	0.1241	-21.97	-1.57
33	0.17876	-0.19177	0.1164	-17.01	-1.67
34	0.12777	-0.17870	0.1089	-11.71	-1.76
35	0.07796	-0.17085	0.1016	-6.07	-1.95
36	0.02854	-0.16813	0.0944	-0.22	-2.06
37	-0.01665	-0.17020	0.0861	5.65	-2.26
38	-0.05857	-0.17677	0.0760	12.42	-2.79
39	-0.09300	-0.18664	0.0639	19.99	-3.69
40	-0.12012	-0.19849	0.0459	26.55	-3.87
41	-0.13680	-0.20681	0.0000	-157.28	340.71
42	-0.14702	-0.20871	0.1226	-178.36	35.39
43	-0.15566	-0.20682	0.3092	-206.49	55.51
44	-0.16179	-0.20179	0.4975	128.50	-737.44
45	-0.16561	-0.19456	0.6577	108.04	43.63
46	-0.16703	-0.18596	0.7617	91.64	32.86
47	-0.16620	-0.17619	0.7992	79.68	21.28
48	-0.16330	-0.16524	0.8136	71.27	12.97
49	-0.15848	-0.15340	0.8269	64.80	8.83
50	-0.15327	-0.14291	0.8427	59.47	7.94

51	-0.14505	-0.13021	0.8607	54.81	5.37
52	-0.13534	-0.11750	0.8805	50.59	4.61
53	-0.12449	-0.10519	0.8999	46.66	4.18
54	-0.11254	-0.09331	0.9189	42.96	3.83
55	-0.09991	-0.08222	0.9366	39.45	3.65
56	-0.08652	-0.07182	0.9539	36.09	3.46
57	-0.07274	-0.06245	0.9705	32.84	3.40
58	-0.05830	-0.05395	0.9857	29.70	3.28
59	-0.04431	-0.04611	0.9950	26.65	3.31
60	-0.02990	-0.03919	1.0136	23.72	3.20
61	-0.01823	-0.03437	1.0226	21.36	3.27
62	-0.00648	-0.03007	1.0269	19.09	3.17
63	0.00531	-0.02626	1.0459	16.60	3.51
64	0.01663	-0.02313	1.0441	14.51	3.10
65	0.02880	-0.02020	1.0530	12.23	3.18
66	0.04059	-0.01790	1.0670	9.86	3.44
67	0.05117	-0.01625	1.0613	7.88	3.24
68	0.06254	-0.01490	1.0664	5.71	3.30
69	0.07418	-0.01397	1.0712	3.58	3.18
70	0.08543	-0.01346	1.0728	1.55	3.14
71	0.09666	-0.01338	1.0832	-0.65	3.42
72	0.10784	-0.01371	1.0885	-2.71	3.22
73	0.11892	-0.01443	1.0942	-4.75	3.21
74	0.12981	-0.01553	1.1007	-6.79	3.24
75	0.14073	-0.01702	1.1053	-8.74	3.10
76	0.15120	-0.01881	1.1084	-10.65	3.12
77	0.16170	-0.02097	1.1125	-12.54	3.08
78	0.17225	-0.02351	1.1175	-14.43	3.03
79	0.18218	-0.02611	1.1148	-16.00	2.67
80	0.19262	-0.02937	1.1259	-18.01	3.21
81	0.20262	-0.03280	1.1309	-19.78	2.92
82	0.21266	-0.03658	1.1377	-21.55	2.88
83	0.22263	-0.04071	1.1487	-23.38	2.97
84	0.23258	-0.04519	1.1533	-25.03	2.64
85	0.24292	-0.05019	1.1620	-26.75	2.61
86	0.25215	-0.05501	1.1605	-28.20	2.42
87	0.26040	-0.05956	1.1608	-29.64	2.68
88	0.26924	-0.06474	1.1630	-31.08	2.45
89	0.27840	-0.07042	1.1654	-32.48	2.27
90	0.28748	-0.07637	1.1718	-33.96	2.37
91	0.29651	-0.08258	1.1725	-35.24	2.05
92	0.30548	-0.08911	1.1788	-36.64	2.20
93	0.31437	-0.09589	1.1830	-37.95	2.04
94	0.32320	-0.10294	1.1871	-39.22	1.96
95	0.33199	-0.11027	1.1914	-40.46	1.89
96	0.34075	-0.11791	1.1961	-41.67	1.83
97	0.34949	-0.12585	1.2016	-42.88	1.78
98	0.35824	-0.13415	1.2070	-44.05	1.69
99	0.36701	-0.14279	1.2104	-45.14	1.55
100	0.37582	-0.15180	1.2122	-46.17	1.43
101	0.38464	-0.16116	1.2129	-47.15	1.33
102	0.39353	-0.17090	1.2126	-48.08	1.23
103	0.40247	-0.18101	1.2111	-48.96	1.14
104	0.41143	-0.19146	1.2084	-49.80	1.07

105	0.42031	-0.20213	1.2044	-50.61	1.01
106	0.42894	-0.21277	1.1992	-51.37	0.97
107	0.43738	-0.22349	1.1931	-52.10	0.94
108	0.44588	-0.23454	1.1864	-52.82	0.90
109	0.45440	-0.24592	1.1791	-53.53	0.87
110	0.46281	-0.25744	1.1711	-54.22	0.85
111	0.47090	-0.26881	1.1624	-54.89	0.84
112	0.47852	-0.27979	1.1528	-55.55	0.86
113	0.48547	-0.29004	1.1423	-56.18	0.89
114	0.49156	-0.29922	1.1308	-56.78	0.95
115	0.49671	-0.30717	1.1183	-57.34	1.03
116	0.50094	-0.31385	1.1052	-57.86	1.15
117	0.50446	-0.31949	1.0917	-58.35	1.29
118	0.50753	-0.32451	1.0774	-58.82	1.38
119	0.51040	-0.32930	1.0623	-59.27	1.42
120	0.53431	-0.37315	0.9470	-62.25	1.04
121	0.54934	-0.40266	0.8911	-63.65	0.74
122	0.56465	-0.43432	0.8356	-64.62	0.48
123	0.57978	-0.46660	0.7885	-65.07	0.22
124	0.59507	-0.49955	0.7501	-65.11	0.02
125	0.60973	-0.53101	0.7198	-64.86	-0.13
126	0.62426	-0.56171	0.6958	-64.44	-0.22
127	0.63776	-0.58962	0.6766	-63.93	-0.29
128	0.65079	-0.61593	0.6608	-63.36	-0.34
129	0.66244	-0.63886	0.6479	-62.75	-0.41
130	0.67340	-0.65985	0.6373	-62.12	-0.46
131	0.68276	-0.67732	0.6288	-61.50	-0.55
132	0.69130	-0.69287	0.6221	-60.91	-0.58
133	0.69818	-0.70509	0.6169	-60.36	-0.68
134	0.70421	-0.71559	0.6128	-59.88	-0.69
135	0.70862	-0.72312	0.6099	-59.48	-0.80
136	0.71226	-0.72926	0.6077	-59.18	-0.73
137	0.71438	-0.73281	0.6063	-59.00	-0.77
138	0.71587	-0.73528	0.6054	-58.98	-0.13
139	0.71603	-0.73554	0.6051	-59.18	11.70

1

#### BOUNDARY LAYER CORRECTION

#### PRESSURE SIDE

N	X	Y	EM	TH	SEP
41	-0.13680	-0.20681	0.00002		
40	-0.12012	-0.19849	0.04592		
39	-0.09300	-0.18664	0.06390		
38	-0.05857	-0.17677	0.07605		
37	-0.01665	-0.17020	0.08611		
36	0.02854	-0.16813	0.09444		
35	0.07796	-0.17085	0.10161		
34	0.12777	-0.17870	0.10893		

33	0.17876	-0.19177	0.11641			
32	0.22754	-0.20907	0.12414			
31	0.27545	-0.23074	0.13214			
30	0.31967	-0.25525	0.14071			
29	0.36172	-0.28299	0.15002			
28	0.39933	-0.31200	0.16032			
27	0.43417	-0.34287	0.17171	0.00093	0.00009	
26	0.46455	-0.37347	0.18434	0.00083	-0.00138	
25	0.49224	-0.40469	0.19815	0.00082	-0.00145	
24	0.51606	-0.43447	0.21310	0.00079	-0.00149	
23	0.53772	-0.46404	0.22894	0.00077	-0.00152	
22	0.55634	-0.49158	0.24552	0.00074	-0.00152	
21	0.57339	-0.51855	0.26258	0.00072	-0.00157	
20	0.58804	-0.54330	0.28128	0.00069	-0.00161	
19	0.60155	-0.56724	0.30066	0.00067	-0.00153	
18	0.61338	-0.58888	0.31789	0.00066	-0.00144	
17	0.62454	-0.60997	0.33467	0.00067	-0.00151	
16	0.63417	-0.62901	0.35328	0.00065	-0.00168	
15	0.64312	-0.64742	0.37453	0.00063	-0.00181	
14	0.65078	-0.66364	0.39670	0.00060	-0.00183	
13	0.65801	-0.67915	0.41858	0.00059	-0.00187	
12	0.66420	-0.69259	0.44112	0.00057	-0.00195	
11	0.67007	-0.70534	0.46444	0.00055	-0.00206	
10	0.67503	-0.71606	0.48812	0.00054	-0.00212	
9	0.67978	-0.72612	0.51136	0.00052	-0.00218	
8	0.68369	-0.73423	0.53336	0.00051	-0.00218	
7	0.68743	-0.74171	0.55346	0.00050	-0.00221	
6	0.69032	-0.74733	0.57100	0.00050	-0.00216	
5	0.69300	-0.75233	0.58549	0.00049	-0.00221	
4	0.69475	-0.75548	0.59628	0.00049	-0.00202	
3	0.69618	-0.75798	0.60301	0.00049	-0.00233	
2	0.69651	-0.75853	0.60508	0.00049	-0.00245	
1	0.69651	-0.75853	0.60508	0.00049	-0.00245	

### SUCTION SIDE

N	X	Y	EM	TH	SEP
42	-0.14702	-0.20871	0.12256		
43	-0.15566	-0.20682	0.30920		
44	-0.16179	-0.20179	0.49755		
45	-0.16561	-0.19456	0.65766		
46	-0.16703	-0.18596	0.76166		
47	-0.16620	-0.17619	0.79923		
48	-0.16330	-0.16524	0.81362		
49	-0.15848	-0.15340	0.82693		
50	-0.15327	-0.14291	0.84271		
51	-0.14505	-0.13021	0.86075		
52	-0.13534	-0.11750	0.88047		
53	-0.12449	-0.10519	0.89992		
54	-0.11254	-0.09331	0.91891		
55	-0.09991	-0.08222	0.93665		

56	-0.08652	-0.07182	0.95393		
57	-0.07274	-0.06245	0.97048		
58	-0.05830	-0.05395	0.98572		
59	-0.04431	-0.04611	0.99495		
60	-0.02990	-0.03919	1.01359		
61	-0.01823	-0.03437	1.02259		
62	-0.00648	-0.03007	1.02691		
63	0.00531	-0.02626	1.04591		
64	0.01663	-0.02313	1.04410		
65	0.02880	-0.02020	1.05301		
66	0.04059	-0.01790	1.06700		
67	0.05117	-0.01625	1.06130		
68	0.06254	-0.01490	1.06638		
69	0.07418	-0.01397	1.07117		
70	0.08543	-0.01346	1.07282		
71	0.09666	-0.01338	1.08317		
72	0.10784	-0.01371	1.08854		
73	0.11892	-0.01443	1.09421		
74	0.12981	-0.01553	1.10075		
75	0.14073	-0.01702	1.10531		
76	0.15120	-0.01881	1.10840		
77	0.16170	-0.02097	1.11253		
78	0.17225	-0.02351	1.11747		
79	0.18218	-0.02611	1.11480		
80	0.19262	-0.02937	1.12586		
81	0.20262	-0.03280	1.13095		
82	0.21266	-0.03658	1.13771		
83	0.22263	-0.04071	1.14875		
84	0.23258	-0.04519	1.15334		
85	0.24292	-0.05019	1.16203		
86	0.25215	-0.05501	1.16045		
87	0.26040	-0.05956	1.16083		
88	0.26924	-0.06474	1.16301		
89	0.27840	-0.07042	1.16536		
90	0.28748	-0.07637	1.17176		
91	0.29651	-0.08258	1.17254		
92	0.30548	-0.08911	1.17877		
93	0.31437	-0.09589	1.18300		
94	0.32320	-0.10294	1.18709		
95	0.33199	-0.11027	1.19141		
96	0.34075	-0.11791	1.19615		
97	0.34949	-0.12585	1.20161		
98	0.35824	-0.13415	1.20695		
99	0.36701	-0.14279	1.21038	0.00023	0.00005
100	0.37582	-0.15180	1.21222	0.00026	-0.00002
101	0.38464	-0.16116	1.21295	0.00029	-0.00000
102	0.39353	-0.17090	1.21259	0.00033	0.00002
103	0.40247	-0.18101	1.21108	0.00036	0.00004
104	0.41143	-0.19146	1.20840	0.00039	0.00006
105	0.42031	-0.20213	1.20445	0.00042	0.00009
106	0.42894	-0.21277	1.19925	0.00046	0.00013
107	0.43738	-0.22349	1.19313	0.00049	0.00015
108	0.44588	-0.23454	1.18641	0.00052	0.00018
109	0.45440	-0.24592	1.17911	0.00056	0.00021

110	0.46281	-0.25744	1.17113	0.00059	0.00024
111	0.47090	-0.26881	1.16240	0.00063	0.00030
112	0.47852	-0.27979	1.15281	0.00067	0.00037
113	0.48547	-0.29004	1.14229	0.00070	0.00048
114	0.49156	-0.29922	1.13075	0.00074	0.00064
115	0.49671	-0.30717	1.11833	0.00077	0.00085
116	0.50094	-0.31385	1.10525	0.00081	0.00112
117	0.50446	-0.31949	1.09167	0.00084	0.00143
118	0.50753	-0.32451	1.07739	0.00087	0.00173
119	0.51040	-0.32930	1.06228	0.00091	0.00193
120	0.53431	-0.37315	0.94698	0.00125	0.00237
121	0.54934	-0.40266	0.89109	0.00150	0.00263
122	0.56465	-0.43432	0.83560	0.00183	0.00303
123	0.57978	-0.46660	0.78846	0.00220	0.00316
124	0.59507	-0.49955	0.75013	0.00258	0.00318
125	0.60973	-0.53101	0.71981	0.00297	0.00311
126	0.62426	-0.56171	0.69582	0.00334	0.00303
127	0.63776	-0.58962	0.67661	0.00368	0.00299
128	0.65079	-0.61593	0.66084	0.00400	0.00300
129	0.66244	-0.63886	0.64788	0.00429	0.00299
130	0.67340	-0.65985	0.63729	0.00456	0.00296
131	0.68276	-0.67732	0.62882	0.00478	0.00289
132	0.69130	-0.69287	0.62208	0.00497	0.00283
133	0.69818	-0.70509	0.61686	0.00513	0.00274
134	0.70421	-0.71559	0.61283	0.00525	0.00271
135	0.70862	-0.72312	0.60988	0.00535	0.00263
136	0.71226	-0.72926	0.60770	0.00542	0.00271
137	0.71438	-0.73281	0.60631	0.00546	0.00269
138	0.71587	-0.73528	0.60542	0.00549	0.00261
139	0.71603	-0.73554	0.60508	0.00550	0.00261

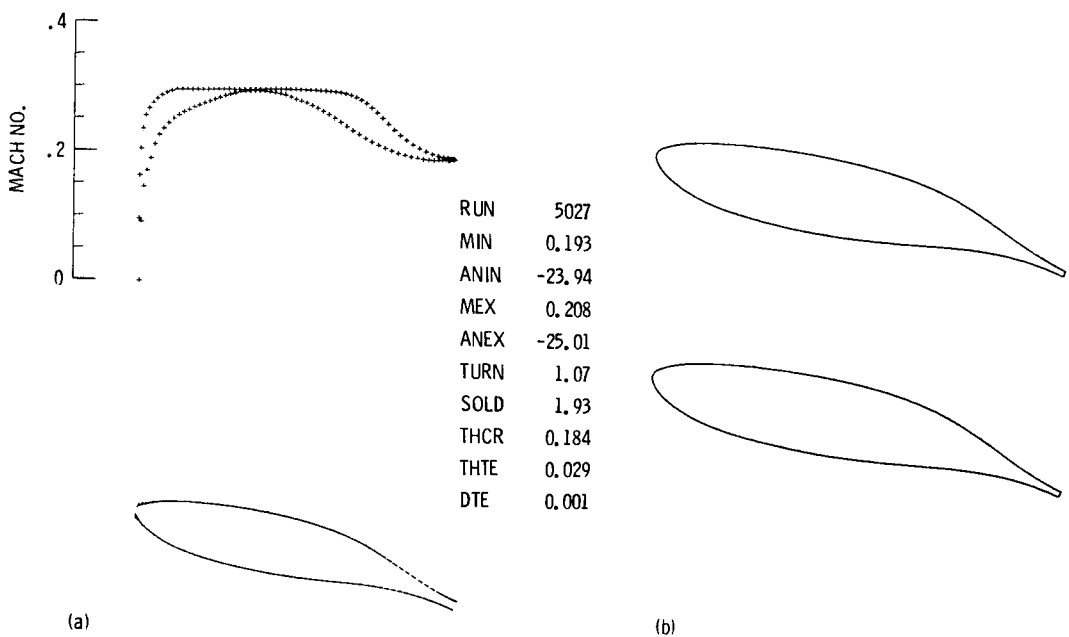
#### BODY COORDINATES AFTER BOUNDARY LAYER SUBTRACTION

N	XV	Y	N	XV	Y
1	0.66279	-0.72097	19	0.57272	-0.53897
2	0.66279	-0.72097	20	0.55988	-0.51620
3	0.66248	-0.72045	21	0.54597	-0.49263
4	0.66113	-0.71808	22	0.52978	-0.46693
5	0.65947	-0.71510	23	0.51208	-0.44071
6	0.65693	-0.71035	24	0.49149	-0.41253
7	0.65418	-0.70501	25	0.46883	-0.38416
8	0.65064	-0.69790	26	0.44256	-0.35435
9	0.64693	-0.69019	27	0.41380	-0.32501
10	0.64243	-0.68063	28	0.37971	-0.29667
11	0.63773	-0.67042	29	0.34395	-0.26909
12	0.63217	-0.65829	30	0.30396	-0.24271
13	0.62630	-0.64550	31	0.26192	-0.21940
14	0.61945	-0.63074	32	0.21636	-0.19880
15	0.61219	-0.61530	33	0.16998	-0.18235
16	0.60371	-0.59777	34	0.12149	-0.16992
17	0.59457	-0.57963	35	0.07413	-0.16246
18	0.58397	-0.55956	36	0.02714	-0.15987

N	XV	Y	N	XV	Y
37	-0.01583	-0.16184	91	0.28194	-0.07853
38	-0.05569	-0.16809	92	0.29047	-0.08473
39	-0.08843	-0.17748	93	0.29893	-0.09118
40	-0.11422	-0.18874	94	0.30732	-0.09788
41	-0.13008	-0.19665	95	0.31568	-0.10485
42	-0.13980	-0.19845	96	0.32401	-0.11212
43	-0.14801	-0.19666	97	0.33232	-0.11967
44	-0.15384	-0.19188	98	0.34064	-0.12756
45	-0.15748	-0.18500	99	0.34863	-0.13613
46	-0.15883	-0.17683	100	0.35690	-0.14479
47	-0.15804	-0.16754	101	0.36524	-0.15372
48	-0.15528	-0.15713	102	0.37364	-0.16302
49	-0.15070	-0.14586	103	0.38208	-0.17266
50	-0.14574	-0.13589	104	0.39054	-0.18263
51	-0.13792	-0.12382	105	0.39893	-0.19280
52	-0.12870	-0.11172	106	0.40707	-0.20296
53	-0.11838	-0.10002	107	0.41504	-0.21317
54	-0.10702	-0.08873	108	0.42306	-0.22371
55	-0.09500	-0.07819	109	0.43110	-0.23457
56	-0.08227	-0.06830	110	0.43903	-0.24554
57	-0.06917	-0.05938	111	0.44666	-0.25638
58	-0.05544	-0.05130	112	0.45385	-0.26684
59	-0.04213	-0.04385	113	0.46039	-0.27662
60	-0.02843	-0.03727	114	0.46611	-0.28537
61	-0.01733	-0.03268	115	0.47095	-0.29295
62	-0.00616	-0.02859	116	0.47491	-0.29933
63	0.00505	-0.02497	117	0.47817	-0.30472
64	0.01581	-0.02200	118	0.48101	-0.30953
65	0.02739	-0.01920	119	0.48315	-0.31442
66	0.03860	-0.01702	120	0.50530	-0.35627
67	0.04866	-0.01545	121	0.51883	-0.38463
68	0.05947	-0.01417	122	0.53257	-0.41505
69	0.07053	-0.01328	123	0.54608	-0.44611
70	0.08123	-0.01280	124	0.55978	-0.47782
71	0.09192	-0.01272	125	0.57300	-0.50810
72	0.10254	-0.01303	126	0.58623	-0.53764
73	0.11308	-0.01372	127	0.59856	-0.56451
74	0.12343	-0.01477	128	0.61053	-0.58984
75	0.13382	-0.01619	129	0.62123	-0.61194
76	0.14378	-0.01789	130	0.63135	-0.63218
77	0.15375	-0.01994	131	0.64001	-0.64905
78	0.16379	-0.02235	132	0.64796	-0.66405
79	0.17323	-0.02483	133	0.65436	-0.67586
80	0.18316	-0.02792	134	0.66003	-0.68600
81	0.19267	-0.03118	135	0.66416	-0.69329
82	0.20221	-0.03479	136	0.66760	-0.69920
83	0.21169	-0.03871	137	0.66961	-0.70263
84	0.22116	-0.04297	138	0.67103	-0.70498
85	0.23098	-0.04773	139	0.67116	-0.70519
86	0.23977	-0.05230			
87	0.24761	-0.05664			
88	0.25601	-0.06156			
89	0.26472	-0.06696			
90	0.27336	-0.07262			

THICK/CHORD AT TE    0.015,    DEV = -0.009

## Turning Vane



(a) Mach number distribution and inviscid airfoil.  
 (b) Relative position of airfoils in cascade plane after boundary layer is subtracted.

Figure 6.—Turning vane.

	N	ARC	V
QDATA			
NRN= 5027			
R= 1.6050	1	-1.457000	-0.800000
EMACH= 0.240	2	-1.229000	-0.837000
THETA= -7.60	3	-1.028000	-0.975000
NI= 3	4	-0.927300	-1.070000
NF= 128	5	-0.814100	-1.153000
GRID= 0.60D-01	6	-0.663500	-1.217000
GRIDS= 0.40D-01	7	-0.571900	-1.231000
IRICH0= 1	8	-0.430300	-1.236000
IRICH0= 0	9	-0.300600	-1.233000
RN= 7000000.0	10	-0.169400	-1.222000
TRU= 0.160	11	-0.050400	-1.113000
TRL= 0.10D0	12	-0.005000	-0.945000
RTH0= 320.0	13	0.009000	-0.825000
QEND	14	0.025000	-0.629400
1	15	0.043000	0.000000
	16	0.069000	0.590000
	17	0.078000	0.630000
	18	0.086000	0.670000

19	0.109200	0.816000
20	0.141600	0.930000
21	0.212100	1.043000
22	0.305800	1.118000
23	0.437200	1.191000
24	0.567800	1.229000
25	0.711500	1.237000
26	0.878700	1.232000
27	1.000000	1.212000
28	1.100000	1.149000
29	1.200000	1.035000
30	1.314000	0.915000
31	1.490000	0.819100
32	1.565000	0.800000

ITER	MIN	ANIN	TURN	GAP	RESID
1	0.19	-23.95	0.61	0.52	-0.1144D 00
2	0.19	-23.94	0.93	0.52	-0.2288D-01
3	0.19	-23.94	1.07	0.52	0.4575D-02

#### INVISCID COMPUTATION

INLET MACH NUMBER = 0.193      INLET FLOW ANGLE = -23.94  
 EXIT MACH NUMBER = 0.208      EXIT FLOW ANGLE = -25.01  
 TURNING = 1.069  
 GAP = 0.522      CHORD = 1.007      AXIAL CHORD = 0.976  
 GAP/CHORD = 0.518      SOLIDITY = 1.931      AXIAL SOLIDITY = 1.870  
 THICK/CHORD = 0.184,      DX = 0.0126; DY = 0.0260  
 THICK/CHORD AT TE = 0.029,      DEV = 0.001

N	X	Y	MACH	ANGL	CURVATURE
1	0.96531	-0.26108	0.1916	-24.50	0.00
2	0.96442	-0.26068	0.1916	-23.93	-10.14
3	0.96027	-0.25888	0.1914	-23.15	-3.01
4	0.95303	-0.25584	0.1912	-22.33	-1.81
5	0.94306	-0.25184	0.1910	-21.44	-1.45
6	0.93074	-0.24713	0.1909	-20.45	-1.31
7	0.91643	-0.24195	0.1910	-19.36	-1.25
8	0.90047	-0.23653	0.1915	-18.16	-1.23
9	0.88315	-0.23106	0.1924	-16.90	-1.22
10	0.86475	-0.22570	0.1937	-15.57	-1.21
11	0.84553	-0.22059	0.1956	-14.22	-1.19
12	0.82570	-0.21581	0.1980	-12.86	-1.16
13	0.80547	-0.21144	0.2010	-11.54	-1.12
14	0.78501	-0.20751	0.2046	-10.27	-1.06
15	0.76448	-0.20401	0.2087	-9.08	-1.00
16	0.74401	-0.20094	0.2132	-7.99	-0.92
17	0.72369	-0.19827	0.2183	-7.02	-0.83
18	0.70362	-0.19595	0.2237	-6.17	-0.73
19	0.68385	-0.19394	0.2295	-5.47	-0.61
20	0.66443	-0.19217	0.2357	-4.94	-0.48
21	0.64539	-0.19059	0.2420	-4.59	-0.32
22	0.62675	-0.18913	0.2483	-4.43	-0.15
23	0.60848	-0.18772	0.2543	-4.44	0.01
24	0.59056	-0.18631	0.2599	-4.57	0.13
25	0.57295	-0.18487	0.2649	-4.78	0.22
26	0.55562	-0.18338	0.2695	-5.05	0.27
27	0.53852	-0.18182	0.2736	-5.37	0.32
28	0.52165	-0.18019	0.2773	-5.72	0.36
29	0.50496	-0.17845	0.2803	-6.13	0.43
30	0.48839	-0.17663	0.2826	-6.37	0.25
31	0.47197	-0.17477	0.2862	-6.61	0.25
32	0.45574	-0.17282	0.2893	-7.17	0.60
33	0.43962	-0.17071	0.2909	-7.69	0.56
34	0.42358	-0.16848	0.2925	-8.15	0.49
35	0.40760	-0.16612	0.2937	-8.54	0.52
36	0.39167	-0.16363	0.2946	-9.11	0.51
37	0.37576	-0.16102	0.2953	-9.59	0.52
38	0.35987	-0.15826	0.2959	-10.07	0.52
39	0.34399	-0.15537	0.2963	-10.57	0.54
40	0.32810	-0.15233	0.2966	-11.07	0.56
41	0.31220	-0.14913	0.2968	-11.65	0.61
42	0.29627	-0.14576	0.2970	-12.25	0.64
43	0.28032	-0.14221	0.2969	-12.90	0.70
44	0.26432	-0.13844	0.2969	-13.60	0.74
45	0.24827	-0.13445	0.2966	-14.36	0.80
46	0.23217	-0.13020	0.2964	-15.17	0.85
47	0.21601	-0.12569	0.2961	-16.06	0.93
48	0.19979	-0.12088	0.2960	-17.03	1.00
49	0.18354	-0.11573	0.2959	-18.12	1.12
50	0.16728	-0.11022	0.2961	-19.37	1.27

51	0.15105	-0.10429	0.2962	-20.84	1.49
52	0.13490	-0.09787	0.2961	-22.55	1.72
53	0.11890	-0.09090	0.2953	-24.55	2.00
54	0.10312	-0.08332	0.2938	-26.82	2.26
55	0.08766	-0.07507	0.2910	-29.38	2.56
56	0.07266	-0.06615	0.2870	-32.19	2.81
57	0.05832	-0.05657	0.2814	-35.33	3.18
58	0.04488	-0.04644	0.2746	-38.81	3.60
59	0.03269	-0.03591	0.2662	-42.97	4.51
60	0.02215	-0.02520	0.2553	-48.33	6.22
61	0.01370	-0.01446	0.2352	-55.64	9.33
62	0.00746	-0.00387	0.2039	-63.60	11.31
63	0.00358	0.00597	0.1631	-74.60	18.16
64	0.00242	0.01466	0.0961	-91.80	34.21
65	0.00435	0.02199	0.0000	65.08	53.23
66	0.00877	0.02812	0.0914	41.75	53.90
67	0.01615	0.03288	0.1451	25.70	31.90
68	0.02606	0.03665	0.1701	17.36	13.74
69	0.03799	0.04000	0.1888	14.52	4.00
70	0.05098	0.04303	0.2109	11.51	3.93
71	0.06465	0.04534	0.2258	7.85	4.61
72	0.07902	0.04697	0.2360	5.20	3.20
73	0.09392	0.04804	0.2439	3.11	2.14
74	0.10943	0.04849	0.2505	1.47	1.84
75	0.12503	0.04870	0.2559	0.09	1.54
76	0.14083	0.04857	0.2606	-1.01	1.21
77	0.15678	0.04815	0.2647	-1.94	1.02
78	0.17282	0.04750	0.2683	-2.67	0.80
79	0.18890	0.04666	0.2718	-3.31	0.69
80	0.20500	0.04565	0.2751	-3.85	0.59
81	0.22106	0.04450	0.2784	-4.37	0.56
82	0.23709	0.04320	0.2814	-4.86	0.53
83	0.25305	0.04177	0.2842	-5.36	0.54
84	0.26894	0.04022	0.2869	-5.85	0.53
85	0.28477	0.03852	0.2891	-6.35	0.55
86	0.30054	0.03670	0.2912	-6.84	0.54
87	0.31625	0.03475	0.2929	-7.33	0.55
88	0.33191	0.03267	0.2943	-7.82	0.54
89	0.34752	0.03045	0.2955	-8.32	0.55
90	0.36310	0.02811	0.2965	-8.81	0.55
91	0.37865	0.02562	0.2971	-9.31	0.55
92	0.39417	0.02301	0.2976	-9.81	0.55
93	0.40968	0.02026	0.2979	-10.31	0.56
94	0.42519	0.01737	0.2980	-10.80	0.54
95	0.44069	0.01434	0.2981	-11.29	0.54
96	0.45619	0.01118	0.2981	-11.81	0.57
97	0.47169	0.00786	0.2981	-12.35	0.60
98	0.48719	0.00439	0.2980	-12.92	0.62
99	0.50269	0.00075	0.2978	-13.52	0.66
100	0.51819	-0.00307	0.2976	-14.16	0.70
101	0.53370	-0.00709	0.2974	-14.85	0.75
102	0.54921	-0.01131	0.2971	-15.60	0.81
103	0.56473	-0.01576	0.2968	-16.41	0.88
104	0.58025	-0.02046	0.2964	-17.31	0.96

105	0.59578	-0.02544	0.2959	-18.30	1.06
106	0.61133	-0.03074	0.2951	-19.39	1.16
107	0.62689	-0.03640	0.2939	-20.58	1.26
108	0.64249	-0.04246	0.2921	-21.88	1.35
109	0.65816	-0.04897	0.2897	-23.28	1.43
110	0.67392	-0.05599	0.2865	-24.75	1.49
111	0.68981	-0.06358	0.2824	-26.28	1.52
112	0.70589	-0.07179	0.2771	-27.82	1.50
113	0.72222	-0.08069	0.2707	-29.32	1.41
114	0.73890	-0.09033	0.2631	-30.67	1.22
115	0.75603	-0.10072	0.2547	-31.79	0.98
116	0.77368	-0.11185	0.2460	-32.62	0.69
117	0.79194	-0.12367	0.2373	-33.13	0.41
118	0.81085	-0.13606	0.2289	-33.31	0.14
119	0.83036	-0.14886	0.2211	-33.16	-0.12
120	0.85036	-0.16183	0.2144	-32.71	-0.33
121	0.87060	-0.17467	0.2087	-32.04	-0.49
122	0.89069	-0.18705	0.2041	-31.22	-0.60
123	0.91010	-0.19861	0.2004	-30.32	-0.70
124	0.92822	-0.20900	0.1975	-29.37	-0.79
125	0.94434	-0.21791	0.1954	-28.42	-0.91
126	0.95782	-0.22506	0.1938	-27.46	-1.09
127	0.96809	-0.23030	0.1927	-26.52	-1.42
128	0.97479	-0.23358	0.1920	-25.61	-2.13
129	0.97775	-0.23498	0.1917	-24.74	-4.63
130	0.97794	-0.23506	0.1916	-24.50	-20.67

1

#### BOUNDARY LAYER CORRECTION

#### PRESSURE SIDE

N	X	Y	EM	TH	SEP
65	0.00435	0.02199	0.00002		
64	0.00242	0.01466	0.09612		
63	0.00358	0.00597	0.16308		
62	0.00746	-0.00387	0.20387		
61	0.01370	-0.01446	0.23515		
60	0.02215	-0.02520	0.25530		
59	0.03269	-0.03591	0.26617		
58	0.04488	-0.04644	0.27463		
57	0.05832	-0.05657	0.28141		
56	0.07266	-0.06615	0.28700		
55	0.08766	-0.07507	0.29101		
54	0.10312	-0.08332	0.29381	0.00003	0.00009
53	0.11890	-0.09090	0.29533	0.00008	-0.00002
52	0.13490	-0.09787	0.29607	0.00013	-0.00001
51	0.15105	-0.10429	0.29617	0.00016	0.00000
50	0.16728	-0.11022	0.29608	0.00019	0.00000

49	0.18354	-0.11573	0.29594	0.00023	0.00000
48	0.19979	-0.12088	0.29600	0.00028	-0.00001
47	0.21601	-0.12569	0.29614	0.00032	-0.00001
46	0.23217	-0.13020	0.29640	0.00035	-0.00002
45	0.24827	-0.13445	0.29664	0.00038	-0.00002
44	0.26432	-0.13844	0.29685	0.00042	-0.00001
43	0.28032	-0.14221	0.29694	0.00045	-0.00000
42	0.29627	-0.14576	0.29696	0.00047	0.00001
41	0.31220	-0.14913	0.29683	0.00050	0.00002
40	0.32810	-0.15233	0.29662	0.00053	0.00003
39	0.34399	-0.15537	0.29629	0.00056	0.00004
38	0.35987	-0.15826	0.29587	0.00058	0.00006
37	0.37576	-0.16102	0.29531	0.00061	0.00008
36	0.39167	-0.16363	0.29461	0.00064	0.00011
35	0.40760	-0.16612	0.29365	0.00067	0.00015
34	0.42358	-0.16848	0.29245	0.00070	0.00021
33	0.43962	-0.17071	0.29090	0.00073	0.00025
32	0.45574	-0.17282	0.28928	0.00077	0.00039
31	0.47197	-0.17477	0.28618	0.00081	0.00059
30	0.48839	-0.17663	0.28262	0.00087	0.00054
29	0.50496	-0.17845	0.28031	0.00091	0.00052
28	0.52165	-0.18019	0.27733	0.00096	0.00071
27	0.53852	-0.18182	0.27359	0.00103	0.00088
26	0.55562	-0.18338	0.26948	0.00110	0.00105
25	0.57295	-0.18487	0.26489	0.00118	0.00126
24	0.59056	-0.18631	0.25986	0.00127	0.00151
23	0.60848	-0.18772	0.25429	0.00139	0.00180
22	0.62675	-0.18913	0.24829	0.00151	0.00210
21	0.64539	-0.19059	0.24201	0.00166	0.00238
20	0.66443	-0.19217	0.23569	0.00183	0.00260
19	0.68385	-0.19394	0.22955	0.00202	0.00276
18	0.70362	-0.19595	0.22373	0.00221	0.00288
17	0.72369	-0.19827	0.21828	0.00242	0.00295
16	0.74401	-0.20094	0.21325	0.00263	0.00297
15	0.76448	-0.20401	0.20867	0.00285	0.00292
14	0.78501	-0.20751	0.20459	0.00307	0.00281
13	0.80547	-0.21144	0.20104	0.00328	0.00261
12	0.82570	-0.21581	0.19805	0.00347	0.00234
11	0.84553	-0.22059	0.19561	0.00364	0.00200
10	0.86475	-0.22570	0.19373	0.00378	0.00161
9	0.88315	-0.23106	0.19237	0.00388	0.00119
8	0.90047	-0.23653	0.19150	0.00396	0.00277
7	0.91643	-0.24195	0.19103	0.00400	0.00037
6	0.93074	-0.24713	0.19090	0.00402	0.00001
5	0.94306	-0.25184	0.19099	0.00402	-0.00029
4	0.95303	-0.25584	0.19121	0.00401	-0.00050
3	0.96027	-0.25888	0.19142	0.00400	-0.00061
2	0.96442	-0.26068	0.19156	0.00399	-0.00064
1	0.96531	-0.26108	0.19164	0.00399	-0.00064

## SUCTION SIDE

N	X	Y	EM	TH	SEP
66	0.00877	0.02812	0.09140		
67	0.01615	0.03288	0.14505		
68	0.02606	0.03665	0.17006		
69	0.03799	0.04000	0.18879		
70	0.05098	0.04303	0.21092		
71	0.06465	0.04534	0.22582		
72	0.07902	0.04697	0.23596		
73	0.09392	0.04804	0.24386		
74	0.10943	0.04849	0.25050		
75	0.12503	0.04870	0.25592		
76	0.14083	0.04857	0.26063		
77	0.15678	0.04815	0.26466		
78	0.17282	0.04750	0.26835	0.00003	0.00009
79	0.18890	0.04666	0.27177	0.00008	-0.00008
80	0.20500	0.04565	0.27515	0.00012	-0.00010
81	0.22106	0.04450	0.27835	0.00015	-0.00011
82	0.23709	0.04320	0.28143	0.00017	-0.00012
83	0.25305	0.04177	0.28425	0.00021	-0.00014
84	0.26894	0.04022	0.28685	0.00025	-0.00014
85	0.28477	0.03852	0.28914	0.00029	-0.00014
86	0.30054	0.03670	0.29116	0.00032	-0.00013
87	0.31625	0.03475	0.29287	0.00036	-0.00012
88	0.33191	0.03267	0.29433	0.00039	-0.00011
89	0.34752	0.03045	0.29551	0.00042	-0.00010
90	0.36310	0.02811	0.29646	0.00045	-0.00008
91	0.37865	0.02562	0.29714	0.00048	-0.00006
92	0.39417	0.02301	0.29764	0.00051	-0.00004
93	0.40968	0.02026	0.29790	0.00054	-0.00002
94	0.42519	0.01737	0.29799	0.00057	-0.00001
95	0.44069	0.01434	0.29808	0.00060	-0.00001
96	0.45619	0.01118	0.29815	0.00063	0.00000
97	0.47169	0.00786	0.29807	0.00066	0.00001
98	0.48719	0.00439	0.29797	0.00068	0.00002
99	0.50269	0.00075	0.29781	0.00071	0.00003
100	0.51819	-0.00307	0.29763	0.00074	0.00003
101	0.53370	-0.00709	0.29740	0.00077	0.00004
102	0.54921	-0.01131	0.29713	0.00080	0.00005
103	0.56473	-0.01576	0.29681	0.00082	0.00006
104	0.58025	-0.02046	0.29642	0.00085	0.00008
105	0.59578	-0.02544	0.29587	0.00088	0.00012
106	0.61133	-0.03074	0.29506	0.00091	0.00019
107	0.62689	-0.03640	0.29385	0.00095	0.00029
108	0.64249	-0.04246	0.29213	0.00099	0.00042
109	0.65816	-0.04897	0.28973	0.00104	0.00059
110	0.67392	-0.05599	0.28654	0.00110	0.00082
111	0.68981	-0.06358	0.28239	0.00117	0.00112
112	0.70589	-0.07179	0.27714	0.00126	0.00151
113	0.72222	-0.08069	0.27067	0.00138	0.00198
114	0.73890	-0.09033	0.26309	0.00153	0.00248

115	0.75603	-0.10072	0.25472	0.00172	0.00297
116	0.77368	-0.11185	0.24598	0.00194	0.00341
117	0.79194	-0.12367	0.23725	0.00220	0.00377
118	0.81085	-0.13606	0.22887	0.00250	0.00402
119	0.83036	-0.14886	0.22114	0.00282	0.00409
120	0.85036	-0.16183	0.21438	0.00316	0.00398
121	0.87060	-0.17467	0.20869	0.00349	0.00373
122	0.89069	-0.18705	0.20406	0.00380	0.00341
123	0.91010	-0.19861	0.20038	0.00407	0.00309
124	0.92822	-0.20900	0.19753	0.00431	0.00280
125	0.94434	-0.21791	0.19536	0.00450	0.00256
126	0.95782	-0.22506	0.19378	0.00465	0.00237
127	0.96809	-0.23030	0.19269	0.00475	0.00226
128	0.97479	-0.23358	0.19202	0.00482	0.00246
129	0.97775	-0.23498	0.19169	0.00485	0.00256
130	0.97794	-0.23506	0.19164	0.00486	0.00256

#### BODY COORDINATES AFTER BOUNDARY LAYER SUBTRACTION

N	XV	Y	N	XV	Y
1	0.96788	-0.25544	31	0.47211	-0.17357
2	0.96694	-0.25500	32	0.45588	-0.17169
3	0.96273	-0.25312	33	0.43976	-0.16966
4	0.95544	-0.24998	34	0.42372	-0.16748
5	0.94542	-0.24583	35	0.40774	-0.16517
6	0.93304	-0.24096	36	0.39181	-0.16273
7	0.91865	-0.23563	37	0.37591	-0.16015
8	0.90258	-0.23009	38	0.36002	-0.15744
9	0.88512	-0.22455	39	0.34413	-0.15459
10	0.86656	-0.21921	40	0.32824	-0.15160
11	0.84715	-0.21420	41	0.31234	-0.14844
12	0.82711	-0.20962	42	0.29641	-0.14511
13	0.80667	-0.20553	43	0.28046	-0.14160
14	0.78602	-0.20195	44	0.26446	-0.13788
15	0.76531	-0.19886	45	0.24841	-0.13393
16	0.74467	-0.19621	46	0.23230	-0.12973
17	0.72422	-0.19397	47	0.21613	-0.12527
18	0.70403	-0.19208	48	0.19991	-0.12050
19	0.68418	-0.19046	49	0.18365	-0.11541
20	0.66470	-0.18907	50	0.16739	-0.10991
21	0.64562	-0.18782	51	0.15115	-0.10402
22	0.62694	-0.18665	52	0.13499	-0.09765
23	0.60865	-0.18549	53	0.11898	-0.09072
24	0.59072	-0.18430	54	0.10314	-0.08327
25	0.57310	-0.18304	55	0.08766	-0.07507
26	0.55576	-0.18170	56	0.07266	-0.06615
27	0.53867	-0.18027	57	0.05832	-0.05657
28	0.52179	-0.17874	58	0.04488	-0.04644
29	0.50510	-0.17710	59	0.03269	-0.03591
30	0.48853	-0.17536	60	0.02215	-0.02520

N	XV	Y	N	XV	Y
61	0.01370	-0.01446	98	0.48699	0.00351
62	0.00746	-0.00387	99	0.50247	-0.00017
63	0.00358	0.00597	100	0.51795	-0.00403
64	0.00242	0.01466	101	0.53344	-0.00807
65	0.00435	0.02199	102	0.54893	-0.01233
66	0.00877	0.02812	103	0.56442	-0.01682
67	0.01615	0.03288	104	0.57991	-0.02156
68	0.02606	0.03665	105	0.59541	-0.02658
69	0.03799	0.04000	106	0.61091	-0.03192
70	0.05098	0.04303	107	0.62643	-0.03763
71	0.06465	0.04534	108	0.64198	-0.04375
72	0.07902	0.04697	109	0.65758	-0.05033
73	0.09392	0.04804	110	0.67325	-0.05744
74	0.10943	0.04849	111	0.68904	-0.06513
75	0.12503	0.04870	112	0.70499	-0.07349
76	0.14083	0.04857	113	0.72116	-0.08258
77	0.15678	0.04815	114	0.73763	-0.09247
78	0.17282	0.04745	115	0.75450	-0.10318
79	0.18889	0.04648	116	0.77186	-0.11471
80	0.20498	0.04544	117	0.78977	-0.12701
81	0.22104	0.04424	118	0.80827	-0.13999
82	0.23706	0.04291	119	0.82736	-0.15346
83	0.25302	0.04148	120	0.84694	-0.16715
84	0.26891	0.03987	121	0.86681	-0.18072
85	0.28473	0.03814	122	0.88660	-0.19379
86	0.30049	0.03628	123	0.90582	-0.20593
87	0.31619	0.03429	124	0.92384	-0.21679
88	0.33184	0.03217	125	0.93995	-0.22602
89	0.34744	0.02992	126	0.95349	-0.23340
90	0.36301	0.02753	127	0.96386	-0.23878
91	0.37855	0.02501	128	0.97068	-0.24214
92	0.39406	0.02236	129	0.97378	-0.24359
93	0.40956	0.01957	130	0.97401	-0.24369
94	0.42505	0.01664			
95	0.44054	0.01358			
96	0.45602	0.01037			
97	0.47150	0.00702			

DXV = 0.0061; DYV = 0.0118

THICK/CHORD AT TE 0.013, DEV = 0.001

## References

1. Sanz, J.M.: Design of Supercritical Cascades with High Solidity. AIAA J., vol. 21, no. 9, Sept. 1983, pp. 1289-1293.
2. Sanz, J.M.: Improved Design of Subcritical and Supercritical Cascades Using Complex Characteristics and Boundary-Layer Correction. AIAA J., vol. 22, no. 7, July 1984, pp. 950-956.
3. Bauer, F.; Garabedian, P.; and Korn, D.: Supercritical Wing Sections III. Springer-Verlag, 1977.
4. Garabedian, P.; and Korn, D.: A Systematic Method for Computer Design of Supercritical Airfoils in Cascade. Comm. Pure Appl. Math, vol. 29, no. 4, 1976, pp. 369-382.
5. Sanz, J.M.: A Well Posed Boundary Value Problem in Transonic Gas Dynamics. Comm. Pure Appl. Math., vol. 31, no 6, 1978, pp. 671-679.
6. Swenson, E.V.: Geometry of the Complex Characteristics in Transonic Flows. Comm. Pure Appl. Math., vol. 21, no. 2, Mar. 1968, pp. 175-185.
7. Green, J.E.; Weeks, D.J.; and Brooman, J.W.F.: Prediction of Turbulent Boundary Layers and Wakes in Compressible Flow by a Lag-Entrainment Method. ARC-R/M-3791, RAE-TR-72231, 1977.
8. Sanz, J.M., et al.: Design and Performance of a Fixed, Nonaccelerating Guide Vane Cascade that Operates Over an Inlet Flow Angle Range of 60 Degrees. J. Eng. Gas Turbines Power, vol. 107, no. 2, Apr. 1985, pp. 477-484.

1. Report No. NASA TP-2676	2. Government Accession No.	3. Recipient's Catalog No.	
4. Title and Subtitle  Lewis Inverse Design Code (LINDES) — Users Manual		5. Report Date  <b>MARCH 1987</b>	
7. Author(s)  Jose M. Sanz	6. Performing Organization Code  505-62-21		
9. Performing Organization Name and Address  National Aeronautics and Space Administration Lewis Research Center Cleveland, Ohio 44135	8. Performing Organization Report No.  E-3221		
12. Sponsoring Agency Name and Address  National Aeronautics and Space Administration Washington, D.C. 20546	10. Work Unit No.		
15. Supplementary Notes	11. Contract or Grant No.		
16. Abstract  The method of complex characteristics and hodograph transformation for the design of shockless airfoils was introduced by Bauer, Garabedian, and Korn and has been extended by the author to design subcritical and supercritical cascades with high solidities and large inlet angles. This new capability was achieved by introducing a new conformal mapping of the hodograph domain onto an ellipse and expanding the solution in terms of Tchebycheff polynomials. A new computer code, the NASA Lewis inverse design code, was developed based on this idea. This new design code is an efficient method for the design of airfoils in cascade. In particular, the design of subcritical cascades of airfoils is a very fast, robust, and versatile process. The inverse design code can be made to interact with a turbulent boundary layer calculation to obtain airfoils with no separated flows at the design condition. This report is intended to serve as a users manual for this design code. Material previously reported by the author is included here for completeness and quick access to the user. The manual contains a description of the method followed by a discussion of the design procedure and examples. The input parameters necessary to run the code are then described and their default values are given. Output listings corresponding to six different blade shapes designed with the code are given, as well as the necessary input data to reproduce the computer runs. The examples have been chosen to show that a wide range of applications can be covered with the code, ranging from supercritical propeller sections to wind tunnel turning vanes that can operate with a large inlet flow angle range.	13. Type of Report and Period Covered  Technical Paper		
17. Key Words (Suggested by Author(s))  Inverse design; Subcritical; Supercritical; Cascades; Turbomachinery; Hodograph; Turning vanes; Boundary layer	18. Distribution Statement  Unclassified—unlimited STAR Category 02		
19. Security Classif. (of this report)  Unclassified	20. Security Classif. (of this page)  Unclassified	21. No of pages  63	22. Price*  A04

\*For sale by the National Technical Information Service, Springfield, Virginia 22161

NASA-Langley, 1987